SAND2019-10198PE

Sandia National Laboratories

Update on Progress Towards Multifluid Electromagnetic Plasma Modeling for Neutral Gas Injection for TDS

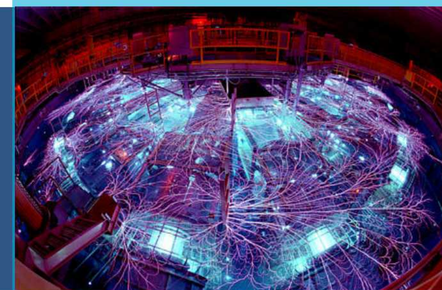

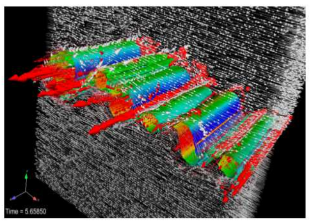

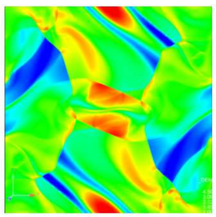

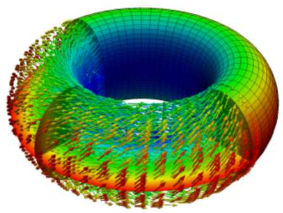

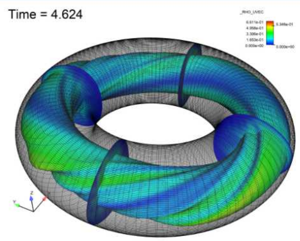

J. N. Shadid, M. M. Crockatt, R. P. Pawlowski, T. M. Smith, S. Conde, W. Hagen, A. Rappport, I. Tomas, T. M. Wilde

Sandia National Laboratories is a multimission laboratory managed and operated by National Technology and Engineering Solutions of Sandia LLC, a wholly owned subsidiary of Honeywell International Inc. for the U.S. Department of Energy's National Nuclear Security Administration under contract DE-NA0003525.

Tokamak Magnetic Confinement Fusion (MCF): Understanding and controlling instabilities/disruptions in plasma confinement is critical.

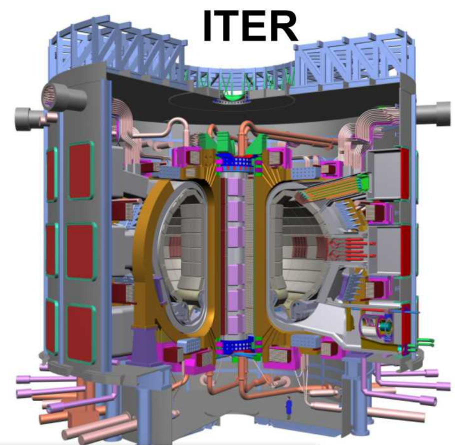

Goal for Fusion Device:

- **Attempt is to achieve temperature of ~100M deg K (6x Sun temp.) ,**
- **Energy confinement times O(1 – 10) min is desired.**

MCF Devices are characterized by large-range of time- and length-scales

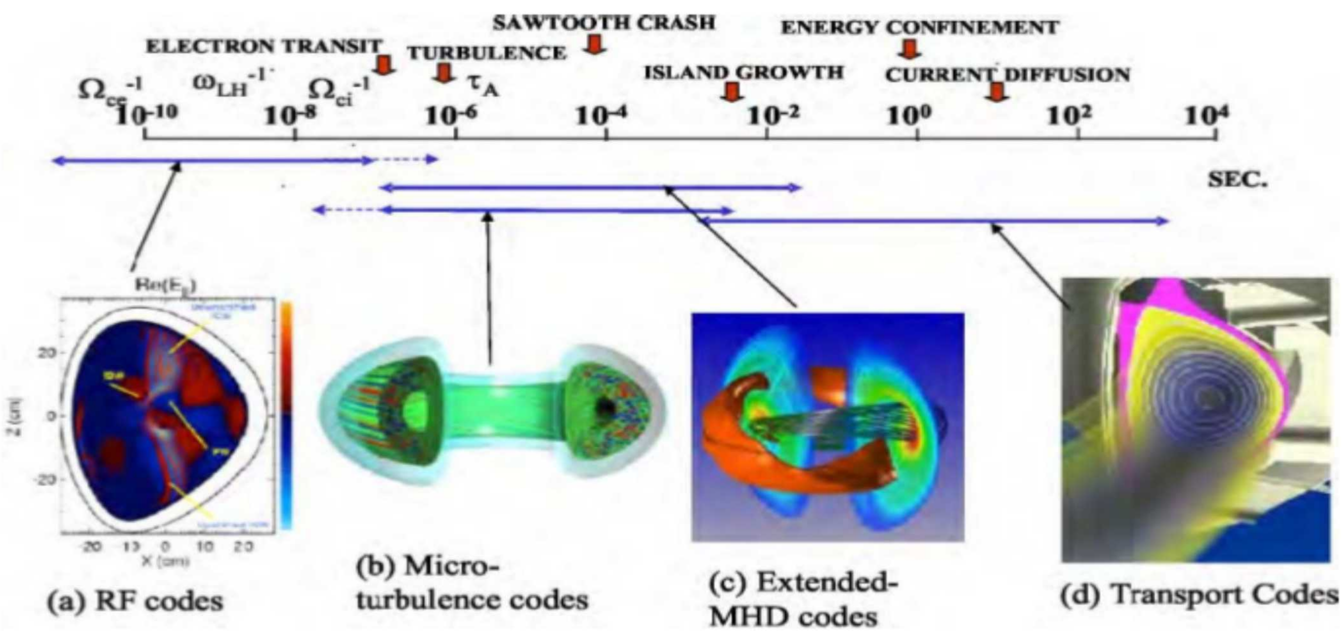

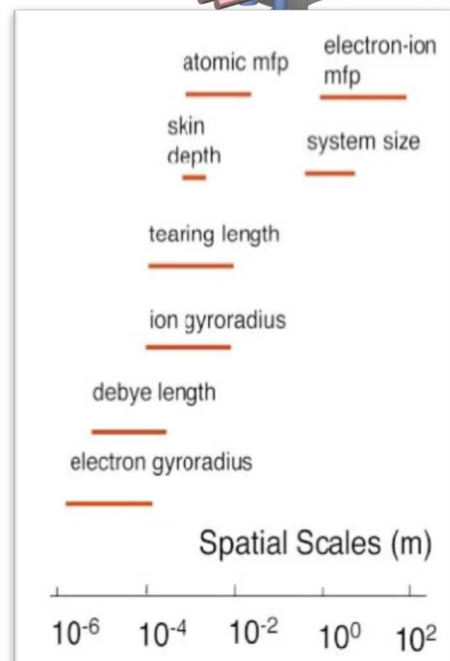

DOE Office of Science ASCR/OFES Reports: Fusion Simulation Project Workshop Report, 2007, Integrated System Modeling Workshop 2015

Our Mathematical Approach - develop:

- Stable, higher-order accurate implicit/IMEX formulations for multiple-time-scale systems
- Stable and accurate unstructured FE spatial discretizations. Options enforcing key mathematical properties (e.g. structure preserving forms: div B = 0; positivity ρ , P; DMP)

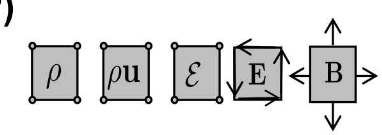

- Robust, efficient fully-coupled nonlinear/linear iterative solution based on Newton-Krylov methods
- Scalable and efficient multiphysics preconditioners utilizing physics-based and approximate block factorization/Schur complement preconditioners with multi-level (AMG) sub-block solvers

=> Also enables beyond forward simulation & integrated UQ (adjoints - error estimates, sensitivities; efficient surrogate modeling (E.g. GP), …)

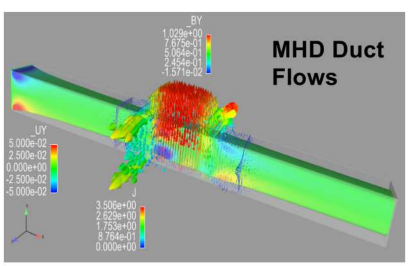

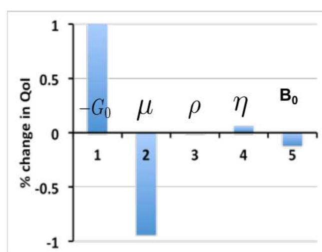

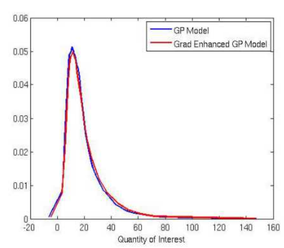

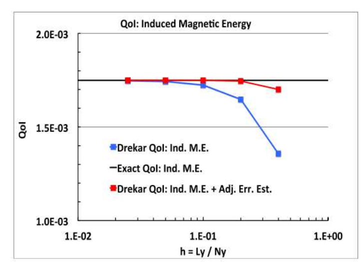

Sandia National Laboratories

3D H(grad) Variational Multiscale (VMS) / AFC formulation

Resistive MHD Model in Residual Notation

$$\frac{\partial \rho \mathbf{v}}{\partial t} + \nabla \cdot [\rho \mathbf{v} \otimes \mathbf{v} - (\mathbf{T} + \mathbf{T}_M)] + 2\rho\Omega \times \mathbf{v} - \rho \mathbf{g} = \mathbf{0}$$

$$\mathbf{T} = -[P - \frac{2}{3}\mu(\nabla \cdot \mathbf{v})]\mathbf{I} + \mu[\nabla \mathbf{v} + \nabla \mathbf{v}^T]$$

$$\mathbf{T_M} \;=\; \frac{1}{\mu_0}\mathbf{B} \otimes \mathbf{B} - \frac{1}{2\mu_0}\|\mathbf{B}\|^2\mathbf{I}$$

$$\frac{\partial \rho}{\partial t} + \nabla \cdot (\rho \mathbf{v}) = 0$$

$$\frac{\partial \Sigma_{tot}}{\partial t} + \nabla \cdot \left[(\rho e + \frac{1}{2}\rho\|\mathbf{u}\|^2)\mathbf{u} + \frac{\mathbf{E} \times \mathbf{B}}{\mu_0} + \mathbf{T} \cdot \mathbf{u} + \mathbf{q} \right] = 0$$

$$\Sigma_{tot} = \rho e + \frac{1}{2}\rho\|\mathbf{u}\|^2 + \|\mathbf{B}\|^2/2\mu_0$$

$$\frac{\partial \mathbf{B}}{\partial t} + \nabla \cdot \left[\mathbf{B} \otimes \mathbf{v} - \mathbf{v} \otimes \mathbf{B} - \frac{\eta}{\mu_0}\left(\nabla \mathbf{B} - (\nabla \mathbf{B})^T\right) + \psi \mathbf{I} \right] = \mathbf{0}$$

$$\frac{1}{c_h}\frac{\partial \psi}{\partial t} + \frac{1}{c_p}\psi + \nabla \cdot \mathbf{B} = 0$$

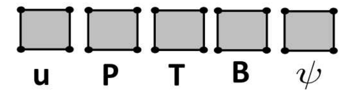

All nodal H(grad) elements using stabilized weak from

- Divergence free involution enforced as constraint with a Lagrange multiplier (Elliptic, parabolic, hyperbolic) [Dedner et. al. 2002; Elliptic: Codina et. al. 2006, 2011, JS et. al. 2010, 2016]
  - Only weakly divergence free in FE implementation (stabilization of B -ψ coupling)
- Can show relationship with projection (e.g. Brackbill and Barnes 1980), and elliptic divergence cleaning (Dedner et. al, 2002) [JS et. al. 2016].
- Issue for using C^0 FE for domains with re-entrant corners / soln singularities [Costabel et. al. 2000, 2002, Codina, 2011, Badia et. al. 2014]

Sandia National Laboratories

Multi-fluid 5-Moment Plasma System Model (Structure-preserving)

Density	$\frac{\partial \rho_a}{\partial t} + \nabla \cdot (\rho_a \mathbf{u}_a) = \sum_{b \neq a} (n_a \rho_b \bar{\nu}^{+}_{ab} - n_b \rho_a \bar{\nu}^{-}_{ab})$
Momentum	$\frac{\partial (\rho_a \mathbf{u}_a)}{\partial t} + \nabla \cdot (\rho_a \mathbf{u}_a \otimes \mathbf{u}_a + p_a I + \Pi_a) = q_a n_a (\mathbf{E} + \mathbf{u}_a \times \mathbf{B})$ $- \sum_{b \neq a} [\rho_a (\mathbf{u}_a - \mathbf{u}_b) n_b \bar{\nu}^{M}_{ab} + \rho_b \mathbf{u}_b n_a \bar{\nu}^{+}_{ab} - \rho_a \mathbf{u}_a n_b \bar{\nu}^{-}_{ab}]$
Energy	$\frac{\partial \varepsilon_a}{\partial t} + \nabla \cdot ((\varepsilon_a + p_a)\mathbf{u}_a + \Pi_a \cdot \mathbf{u}_a + \mathbf{h}_a) = q_a n_a \mathbf{u}_a \cdot \mathbf{E} + Q^{src}$ $- \sum_{b \neq a} \left[(T_a - T_b) k \bar{\nu}^{E}_{ab} - \rho_a \mathbf{u}_a \cdot (\mathbf{u}_a - \mathbf{u}_b) n_b \bar{\nu}^{M}_{ab} \right.$
Charge and Current Density	$q = \sum_k q_k n_k \qquad \mathbf{J} = \sum_k q_k n_k \mathbf{u}_k$
Maxwell's Equations	$\frac{1}{c^2}\frac{\partial \mathbf{E}}{\partial t} - \nabla \times \mathbf{B} + \mu_0 \mathbf{J} = \mathbf{0} \qquad \nabla \cdot \mathbf{E} = \frac{q}{\epsilon_0}$ $\frac{\partial \mathbf{B}}{\partial t} + \nabla \times \mathbf{E} = \mathbf{0} \qquad \nabla \cdot \mathbf{B} = 0$

Cyclotron Frequency

Strong off diagonal coupling for plasma oscillation

Light wave

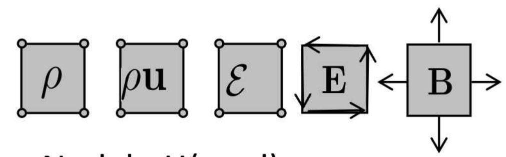

Nodal - H(grad),
Edge - H(curl)
Face - H(div)
Elements
[Intrepid]

IMEX: Time Integration

$$\mathrm{M}\dot{\mathrm{U}} + \mathbf{F} + \mathbf{G} = 0$$

Explicit Hydrodynamics

Implicit EM, EM sources, sources for species $(\rho_a, \rho_a \mathbf{u}_a, \epsilon_a)$ interactions

Other work on mulitfluid formulations, solution algorithms:

See e.g.
Abgral et. al.;
Barth;
Kumar et. al.;
Laguna et. al.; Rossmanith et. al.;
Shumlak et. al.;

Sandia National Laboratories

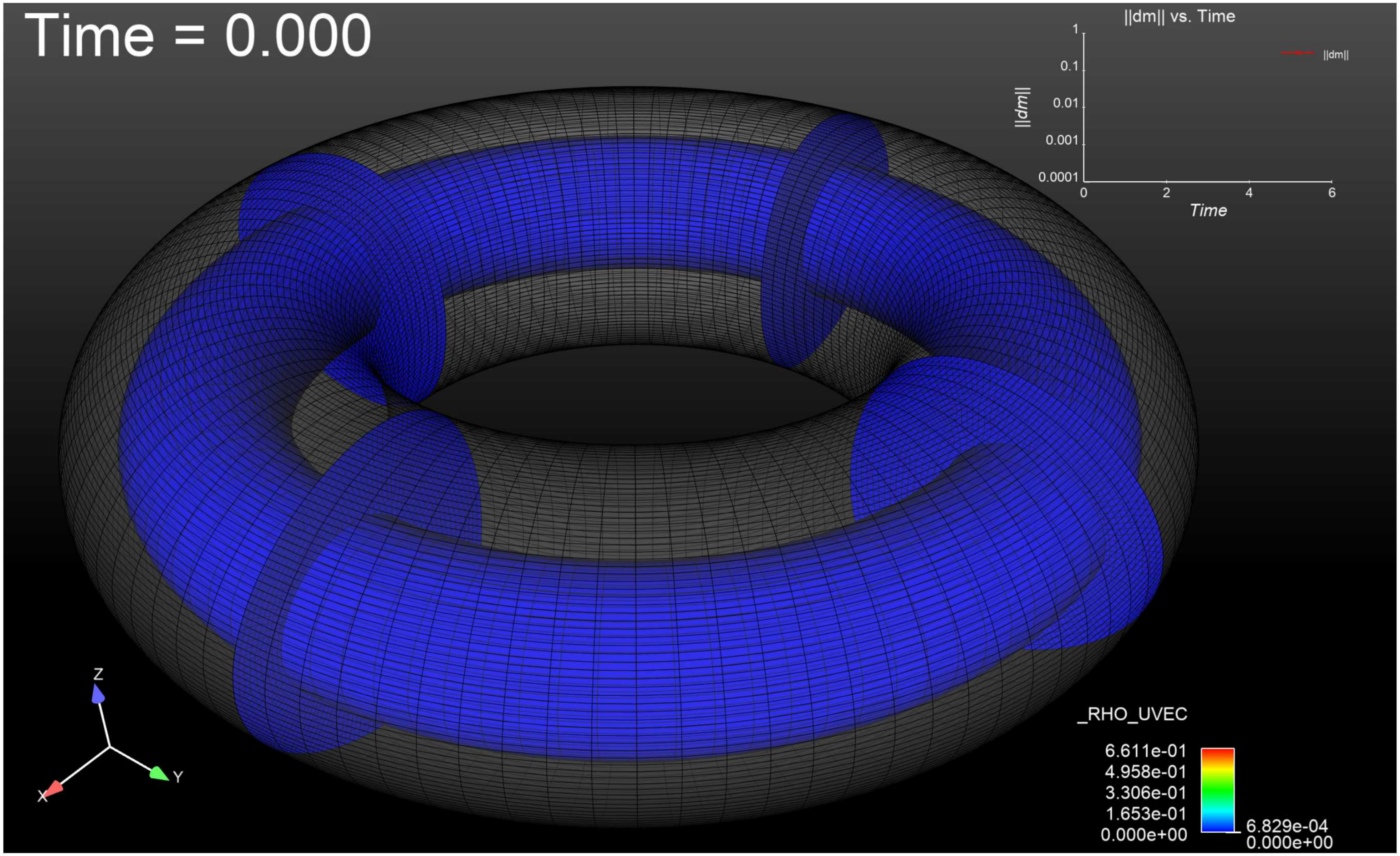

Time = 0.000
||dm|| vs. Time
||dm||
1
0.1
0.01
0.001
0.0001
0
2
4
6
Time
||dm||
_RHO_UVEC
6.611e-01
4.958e-01
3.306e-01
1.653e-01
0.000e+00
6.829e-04
0.000e+00
Z
Y
X

Preliminary Soloveev Nonlinear Disturbance Saturation.

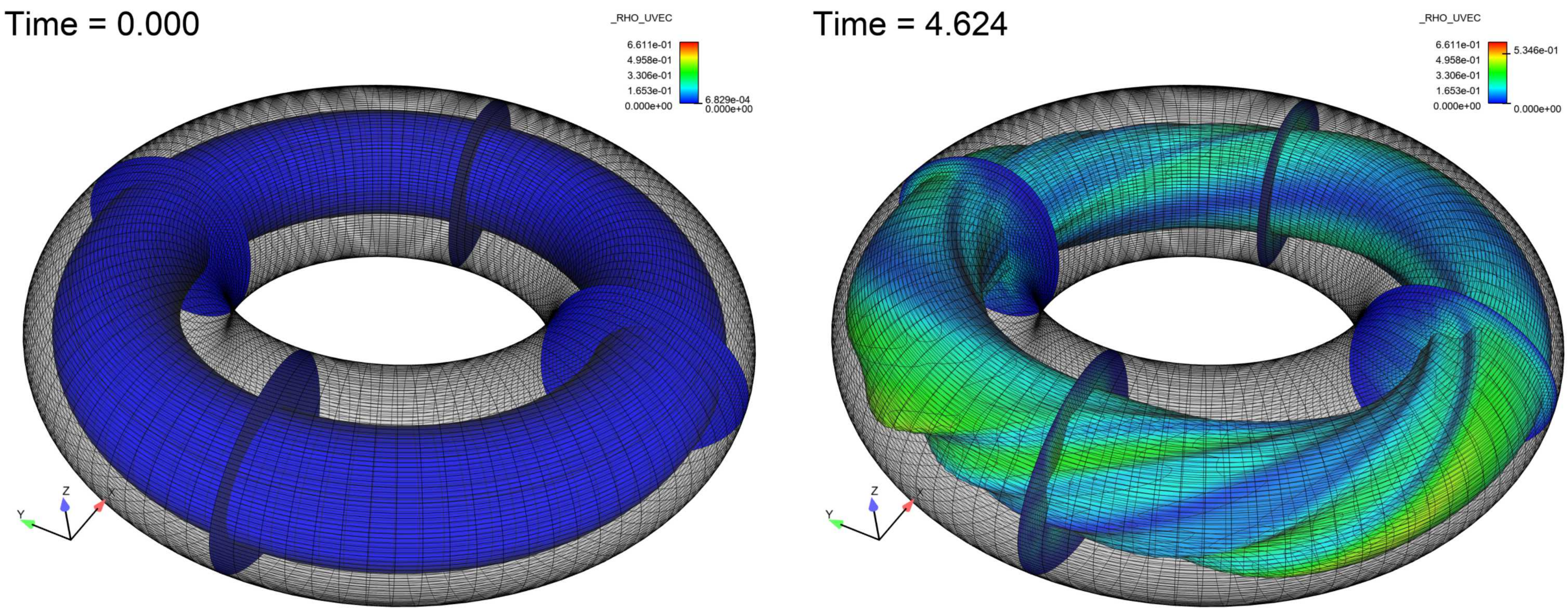

Preliminary Soloveev Equilibrium/Linear Disturbance Growth.

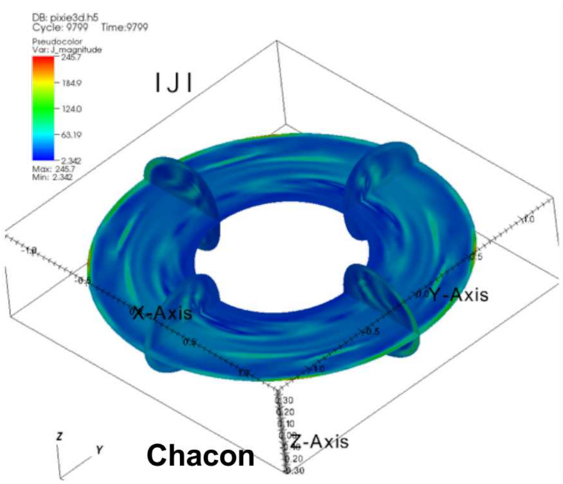

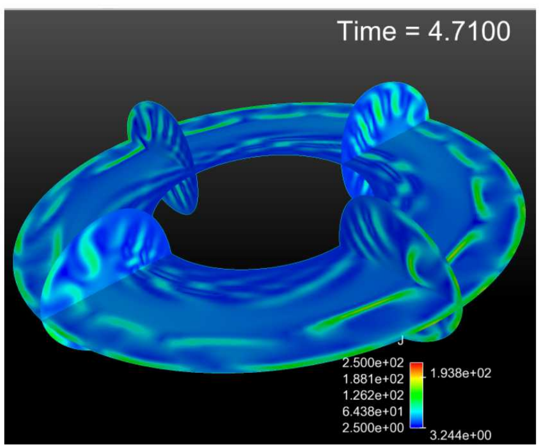

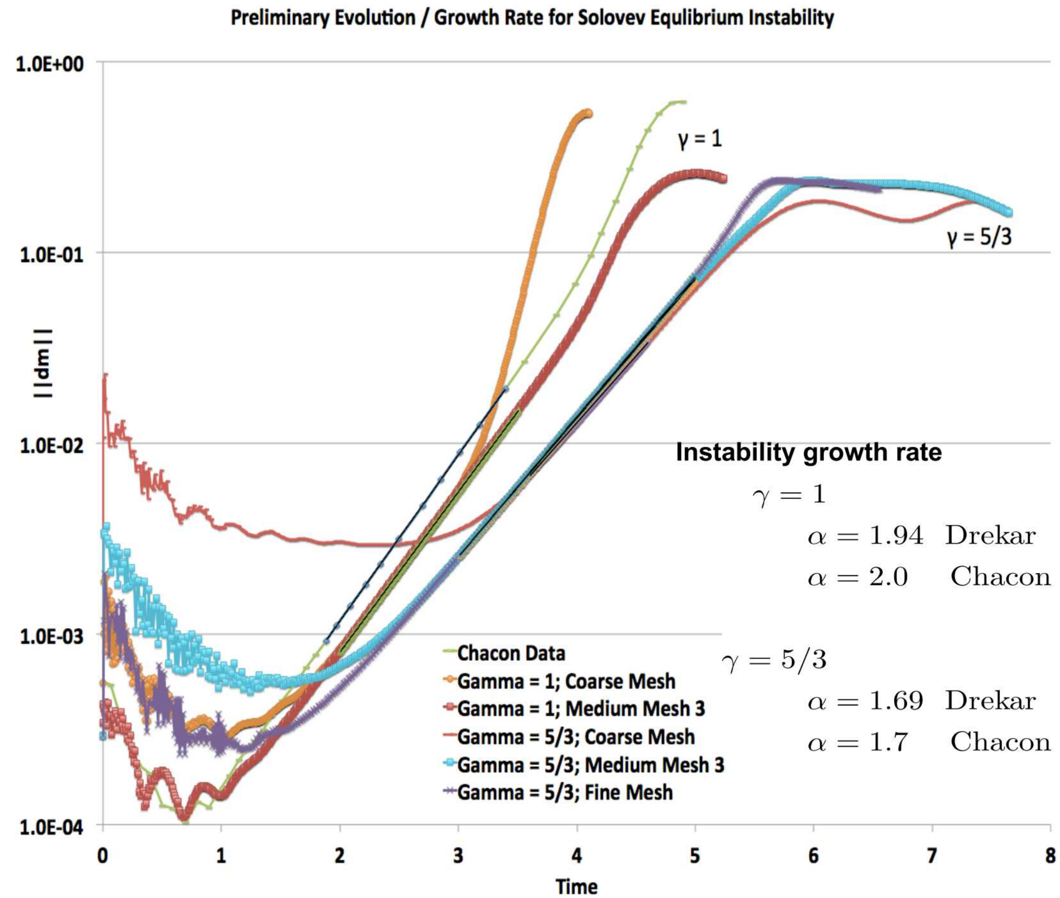

Instability growth rate

$\gamma = 1$

$\alpha = 1.94$ Drekar

$\alpha = 2.0$ Chacon

$\gamma = 5/3$

$\alpha = 1.69$ Drekar

$\alpha = 1.7$ Chacon

with L. Chacon (LANL)

$$\frac{P}{P_0} = (\frac{\rho}{\rho_0})^{\gamma}$$

Sandia National Laboratories

Implicit Methods for Multiple-time-scale systems: E.g. 2D Tearing Mode
Low Mach number compressible; M ~ 10^{-4}; Fully-implicit (BDF2), IMEX (SSP3)

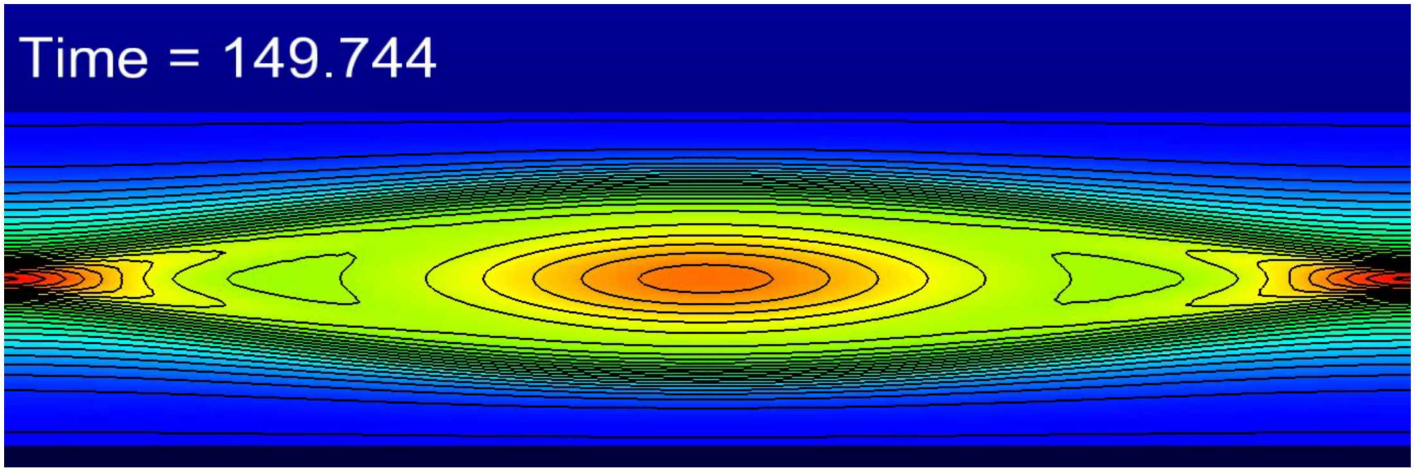

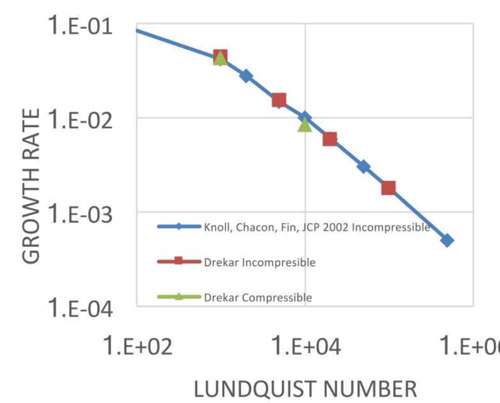

<u>Approx. Computational Time Scales:</u>

- Divergence Constraint ($\nabla \cdot \mathbf{B} = 0$): $1/\infty = 0$
- Fast Magnetosonic Wave (c_f): 10^{-4} to 10^{-2}
- Alfven Wave (c_a): 10^{-4} to 10^{-2}
- Slow Magnetosonic Wave (c_s): 10^{-2} to 10^{-1}
- Sound Wave (c): 10^{-2}
- Advection (c_v): ∞ to 10^{1}
- Diffusion: 10^{-4} to 10^{-2}
- Macroscopic Tearing Mode: 10^{2}

<u>Wave speeds</u>

$$\|\mathbf{u}\|, \|\mathbf{u}\| \pm c_s, \|\mathbf{u}\| \pm c_a, \|\mathbf{u}\| \pm c_f, \pm c_h$$

Fully-implicit (BDF2) / IMEX SSP3
Max CFL:

$CFL_{div} = \infty$
$CFL_{cf} \sim 10^5$ to 10^4
$CFL_{cA} \sim 10^5$ to 10^4
$CFL_{cs} \sim 10^3$ to 10^2
$CFL_{c} \sim 10^3$ to 10^2
$CFL_{cv} \sim 1$ to 0.1

Sandia National Laboratories

Large-scale Scaling Studies for Cray XK7 AND BG/Q; VMS 3D FE MHD

u P B r (similar discretizations for all variables, fully-coupled H(grad) AMG)

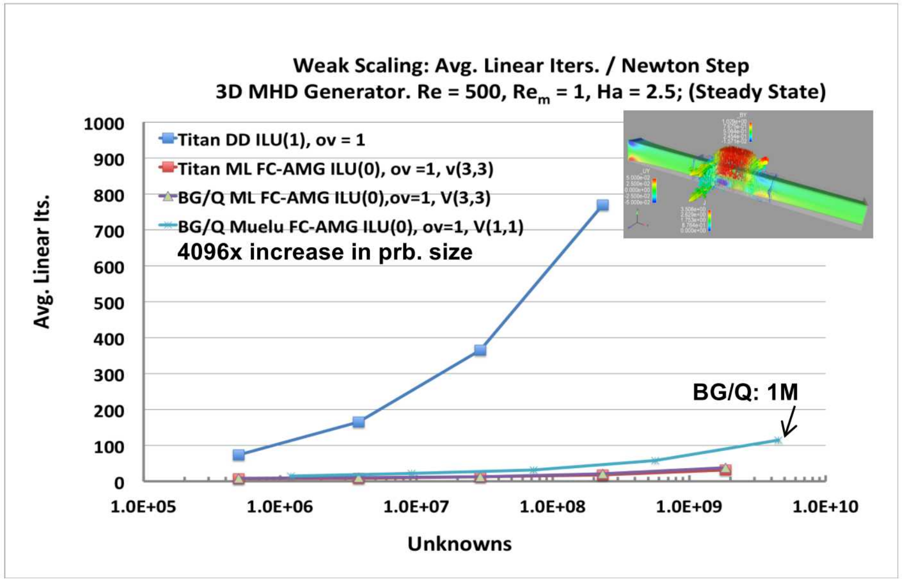

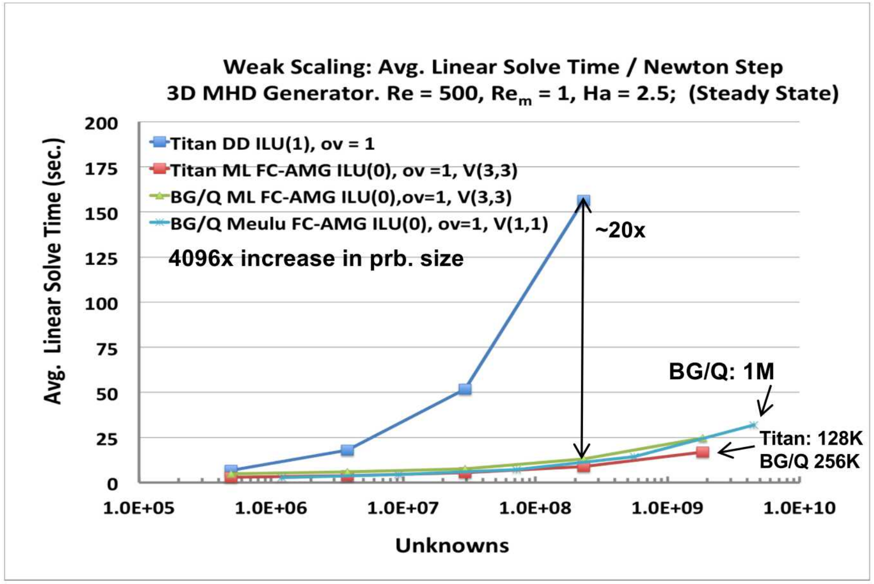

Largest fully-coupled unstructured FE MHD solves demonstrated to date:

MHD (steady) weak scaling studies to 128K Cray XK7, 1M BG/Q
Large demonstration computations

- **MHD (steady): 13B DoF, 1.625B elem, on 128K cores**
- **CFD (Transient): 40B DoF, 10.0B elem, on 128K cores**

Poisson sub-block solvers: 4.1B DoF, 4.1B elem, on 1.6M cores

Sandia National Laboratories

Scaling for VMS 3D Island Coalescence Problem:
Driven Magnetic Reconnection
[$S = 10^3$, dt = 0.1]

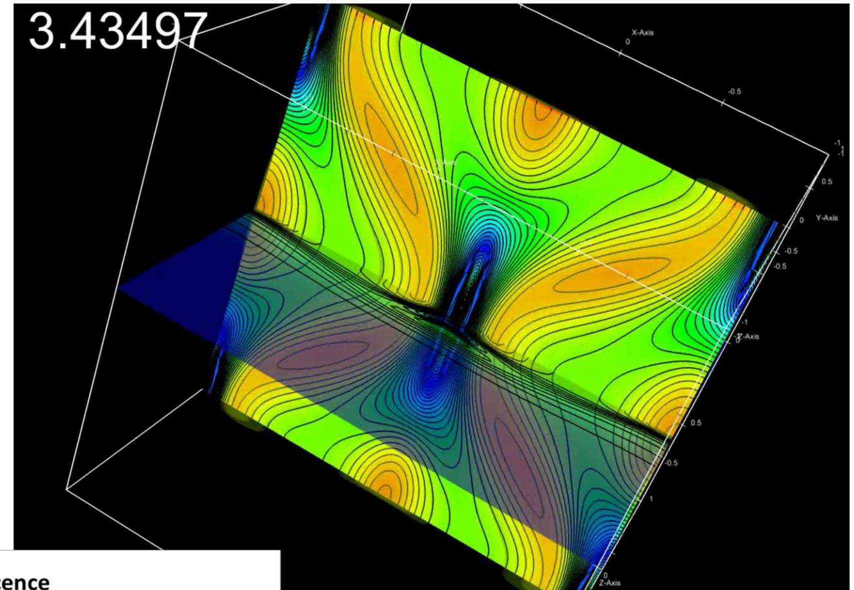

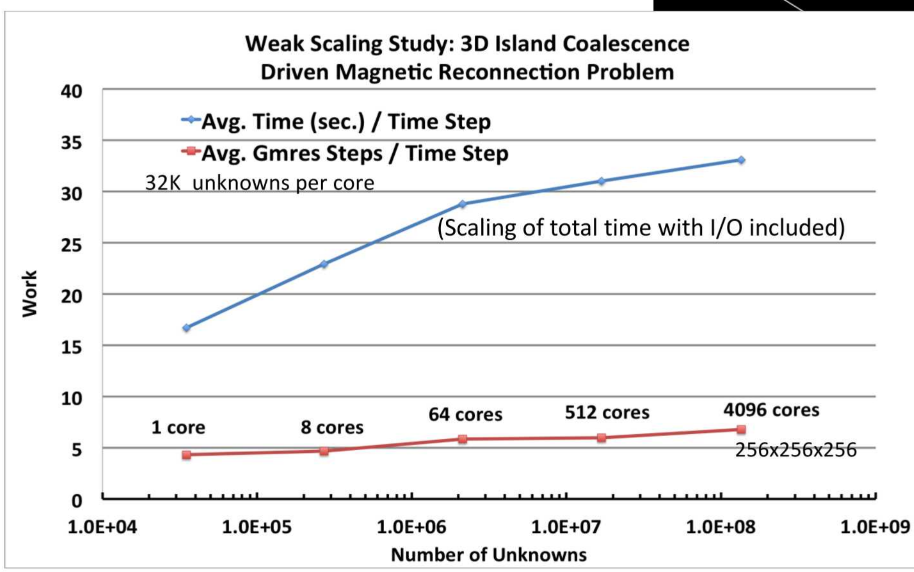

Scaling with Lundquist No.

Lundquist No. S	Newt. Steps / dt	Gmres Steps / dt
1.0E+03	1.36	5.2
5.0E+03	1.43	5.7
1.0E+04	1.51	6
5.0E+04	2	9.8
1.0E+05	2	12
5.0E+05	2	8.4
1.0E+06	2	8.4

BDF2 NK FC-AMG ILU(fill=0,ov=1), V(3,3)
SNL Capacity Cluster: Chama
Mesh: 128x128x128, dt = 0.0333.

Sandia National Laboratories

Demonstration of scalable physics-based preconditioners / solvers for multifluid EM plasmas: 3D Gaussian high density/pressure as initial condition for isentropic ion-acoustic wave propagation

$$\begin{bmatrix} \mathbf{Q}_B & \mathbf{K}_E^B & 0 \\ 0 & \hat{\mathcal{D}}_E & \mathbf{Q}_F^E \\ 0 & 0 & \hat{\mathbf{S}}_F \end{bmatrix} \begin{bmatrix} \mathbf{B} \\ \mathbf{E} \\ \mathbf{F} \end{bmatrix}$$

$$\mathcal{D}^E = \mathrm{Q}_E - \mathrm{K}_B^E \bar{\mathrm{Q}}_B^{-1} \mathrm{K}_E^B \qquad \text{H(curl) AMG}$$

$$\mathbf{S}_F = \mathbf{D}_F - \mathcal{K}_E^F \mathcal{D}_E^{-1} Q_F^E \qquad \text{H(grad) AMG}$$

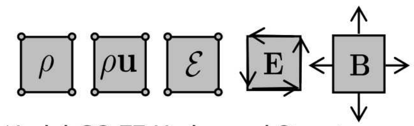

Nodal CG FE Hydro and Structure-preserving discretization for EM

Nodal - H(grad),
Edge - H(curl)
Face - H(div)
Elements
[Intrepid]

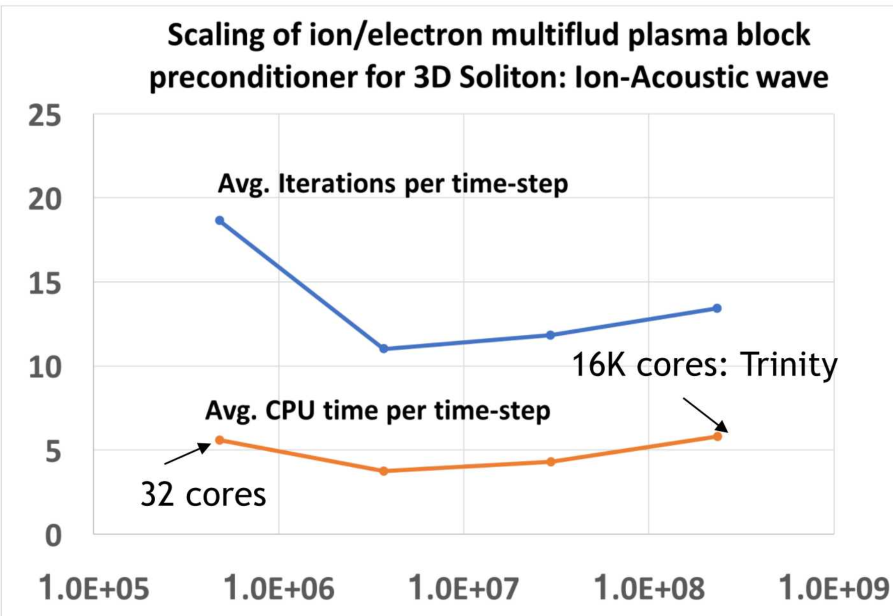

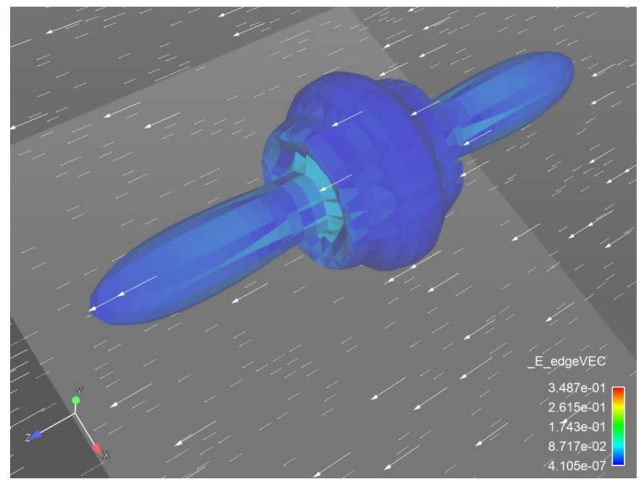

Iso-surface of ion density colored by electric field magnitude

Isentropic flow

$$\frac{P}{P_0} = \left(\frac{\rho}{\rho_0}\right)^{\gamma} \qquad \mu = \frac{m_i}{m_e} = 25$$

3D Plane Jet; Kelvin-Helmholtz Unstable with Secondary Cross-stream Instability;
VMS LES Model; Re = 10^8

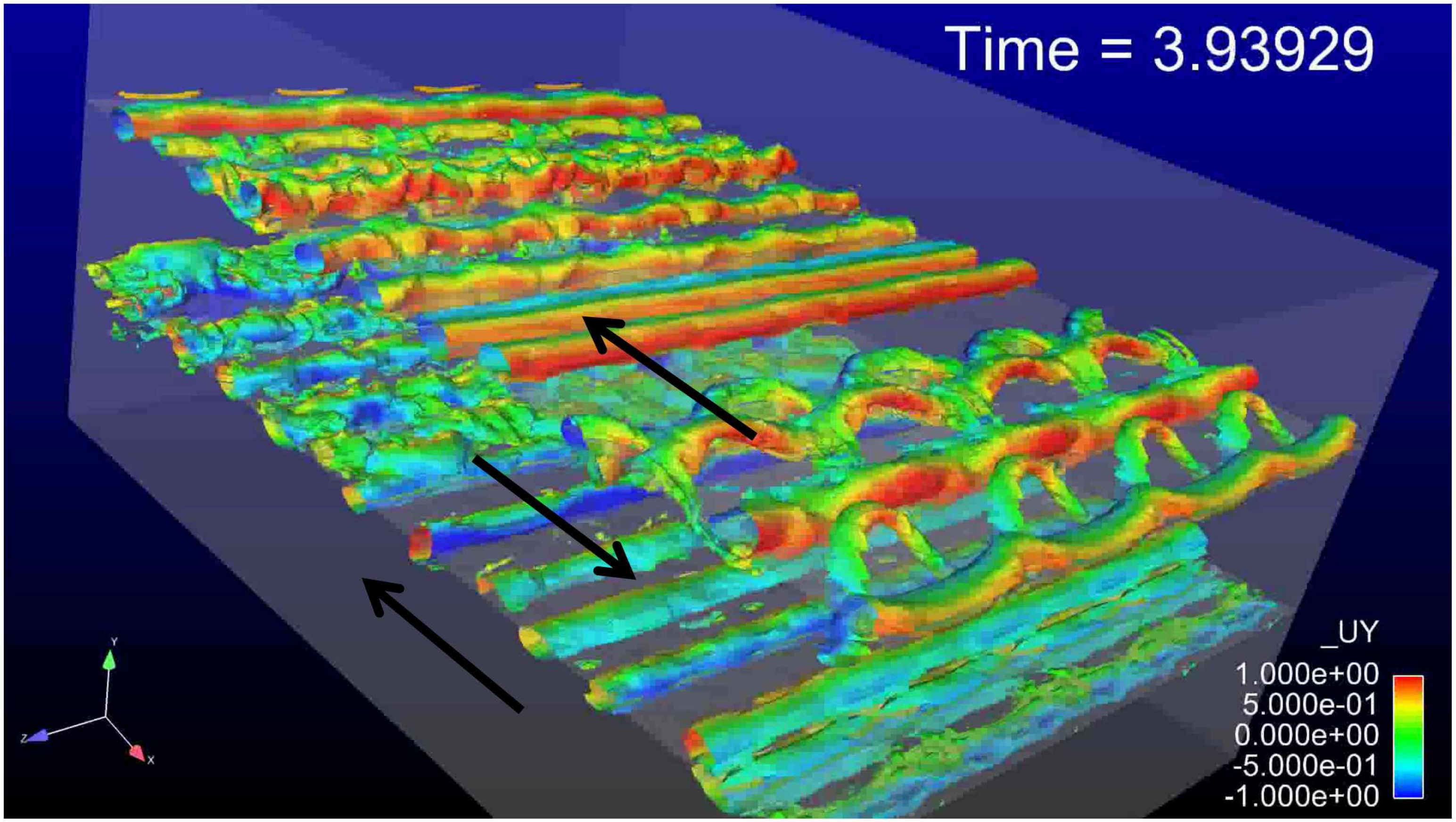

Sandia National Laboratories

VMS LES MHD Model induced cross term fluxes for sub-grid to resolved scale transfers Consistent and dynamic model. MHD Taylor-Green Vortex Decay

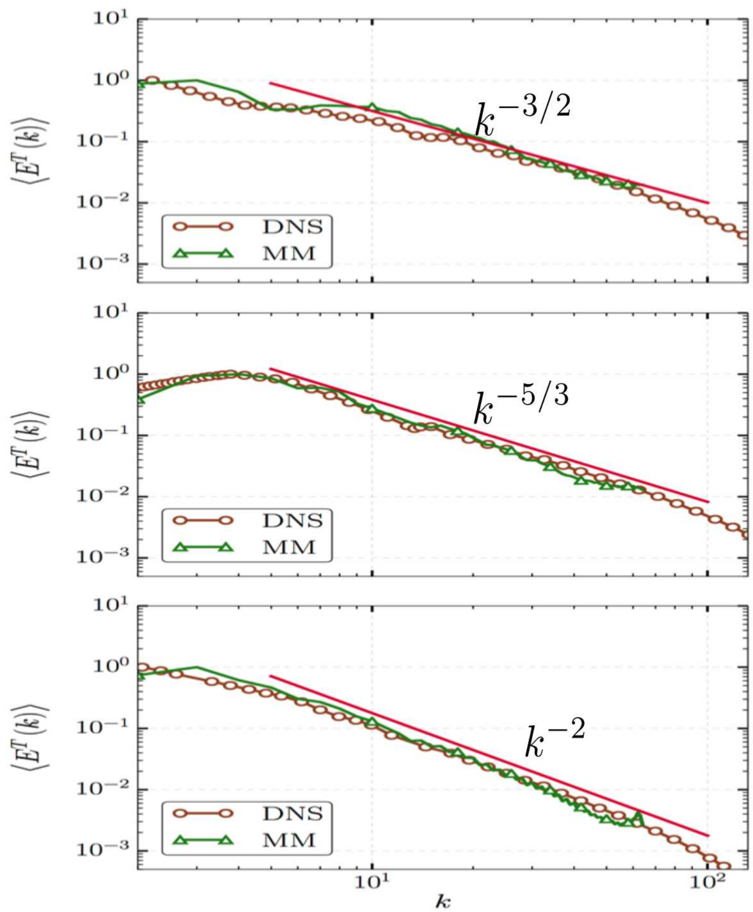

MHD Taylor-Green Vortex Decay: Non-universality of total energy turbulent decay spectrum (MHD VMS–LES)

VMS-LES MHD Turbulence Model – MHD vortex
(w/ A. Oberai- RPI, D. Sondak- Harvard)

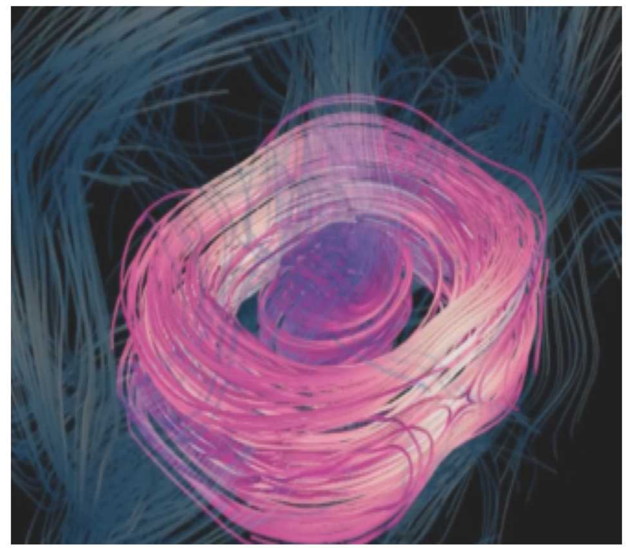

Sandia National Laboratories

Robustness and Accuracy: AFC & Invariant Domain Preserving Methods

AFC local bounds preserving method:
Ideal MHD smooth Alfven wave convergence

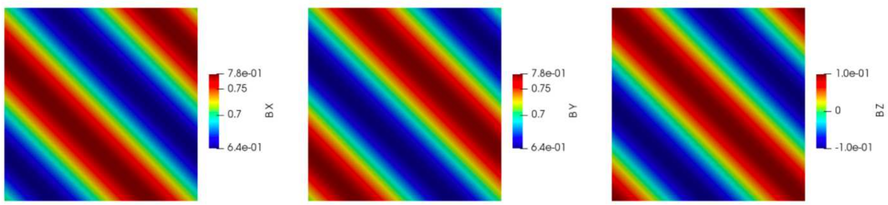

Figure 8: The smooth Aflven wave magnetic field profiles for the solution obtained when segregated limiting based on ρ is applied. The mesh has $\Delta x = \Delta y = \frac{1}{256}$. The time step is $\Delta t = 1.5625 \times 10^{-4}$.

Δx	Δt	L^1	EOC_1	L^2	EOC_2
$\frac{1}{8}$	5×10^{-3}	$9.56965103e-02$	–	$7.49845125e-02$	–
$\frac{1}{16}$	2.5×10^{-3}	$2.80237139e-02$	1.7718	$2.20141990e-02$	1.7681
$\frac{1}{32}$	1.25×10^{-3}	$7.22549121e-03$	1.9554	$5.67504738e-03$	1.9557
$\frac{1}{64}$	6.25×10^{-4}	$1.81897295e-03$	1.9899	$1.42867753e-03$	1.9899
$\frac{1}{128}$	3.125×10^{-4}	$4.55539220e-04$	1.9974	$3.57774759e-04$	1.9975
$\frac{1}{256}$	1.5625×10^{-4}	$1.13931076e-04$	1.9994	$8.94807819e-05$	1.9994

Table 12: The convergence rates for B_y in the smooth Alfven wave test when segregated limiting based on ρ is used.

AFC local bounds preserving method:
Ideal MHD MHD shock tube Ryu-Jones problem.

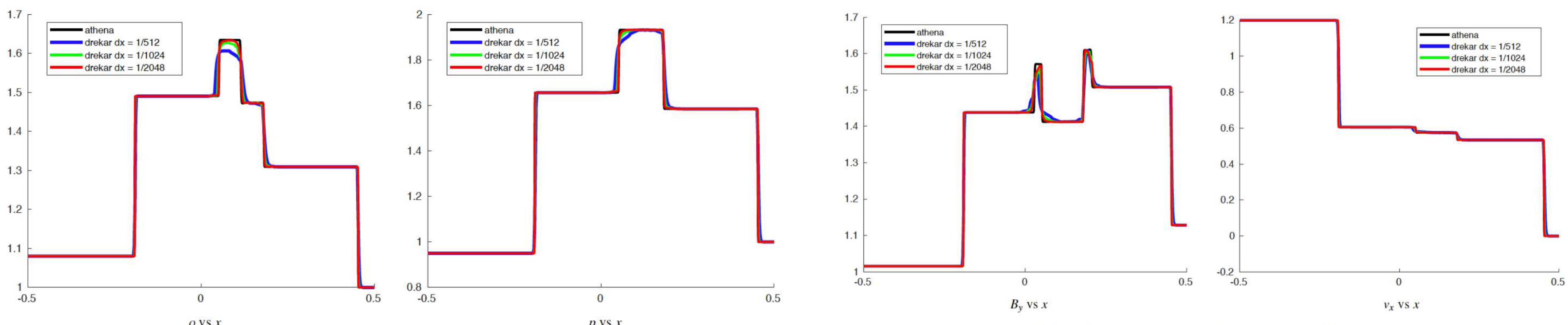

Figure 5: The Ryu-Jones test using $\alpha_e^{\rho}\alpha_e^{\rho p}$ synchronized limiting. The AFC result is compared to a reference solution from the Athena code with mesh $\Delta x = \frac{1}{2000}$ at $T = 0.1$.

AFC Solution: Orszag – Tang Vortex Prb.

Mesh
256x256

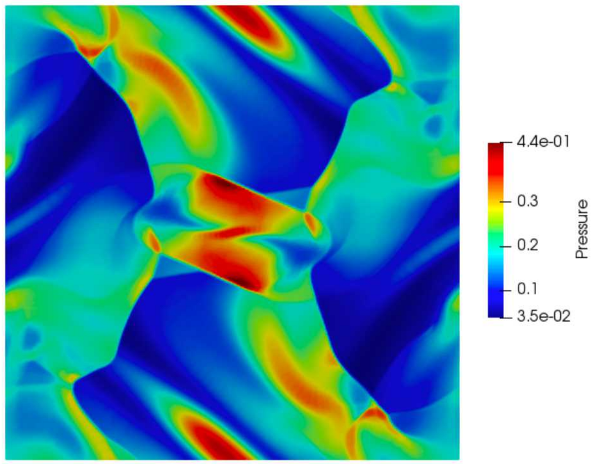

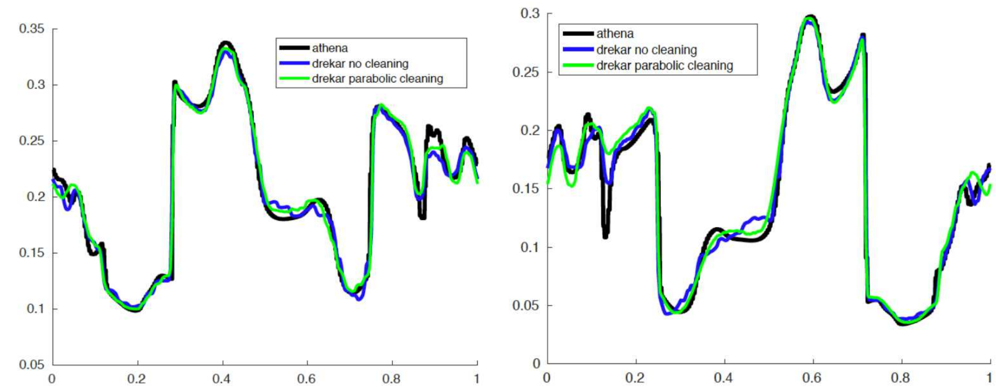

(a) density at $y = 0.75$ (b) pressure at $y = 0.25$

Figure 15: Comparison of the density and pressure trace profiles in the Orszag-Tang problem between **Athena** and the AFC method **no divergence cleaning** and with **parabolic divergence cleaning**. The mesh has $\Delta x = \Delta y = \frac{1}{256}$. The time step is $\Delta t = 10^{-4}$. The profiles are plotted at $T = 0.5$.

Mesh
1024x1204

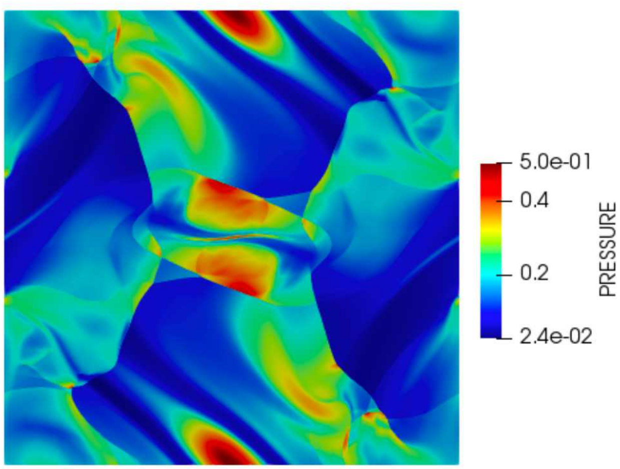

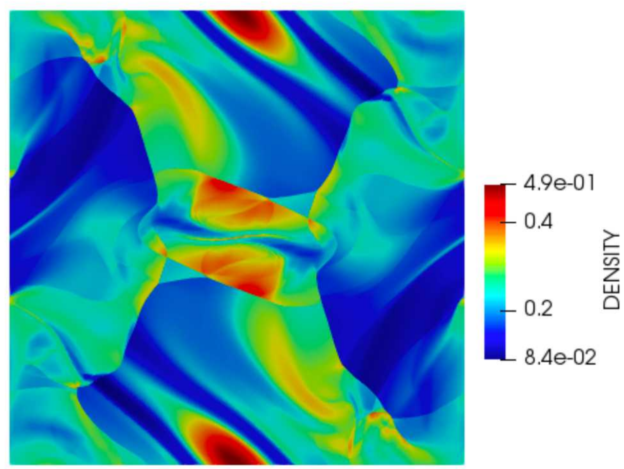

AFC Solution:
Orszag – Tang
Vortex Prb.
1024x1024 mesh

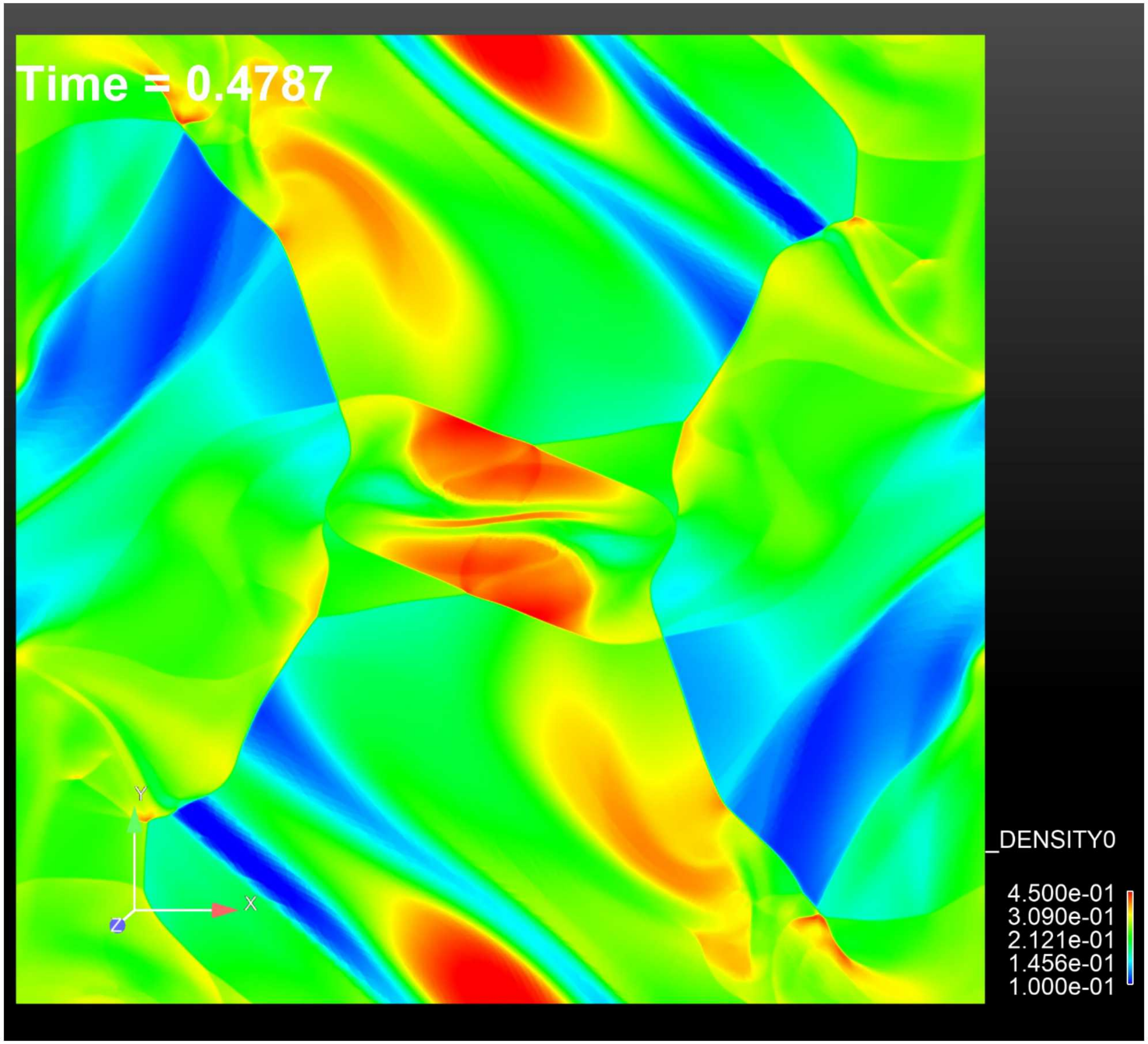

Sandia National Laboratories

Overview of Models and Equations

Kinetic equations:

$$\partial_t f_s + \mathbf{v}\cdot\nabla_{\mathbf{x}} f_s + \frac{q_s}{m_s}(\mathbf{E}+\mathbf{v}\times\mathbf{B})\cdot\nabla_{\mathbf{v}} f_s = \mathcal{C}_s\left[f_s\right] + \mathcal{S}_s, \qquad (s\in\Lambda),$$

with

$$\mathcal{C}_s = \mathcal{C}_s^{\mathrm{sc}} + \mathcal{C}_s^{\mathrm{ion}} + \mathcal{C}_s^{\mathrm{rec}} + \mathcal{C}_s^{\mathrm{cx}} + \mathcal{C}_s^{\mathrm{rad}}.$$

Fluid equations:

$$\begin{aligned}
\partial_t\rho_s + \nabla\cdot\left(\rho_s\mathbf{u}_s\right) &= \mathcal{C}_s^{[0]} + \mathcal{S}_s^{[0]},\\
\partial_t\left(\rho_s\mathbf{u}_s\right) + \nabla\cdot\left(\rho_s\mathbf{u}_s\otimes\mathbf{u}_s + p_s\underline{\mathbf{I}} + \underline{\mathbf{\Pi}}_s\right) &= q_s n_s\left(\mathbf{E}+\mathbf{u}_s\times\mathbf{B}\right) + \boldsymbol{\mathcal{C}}_s^{[1]} + \boldsymbol{\mathcal{S}}_s^{[1]},\\
\partial_t\mathcal{E}_s + \nabla\cdot\left[\left(\mathcal{E}_s+p_s\right)\mathbf{u}_s + \mathbf{u}_s\cdot\underline{\mathbf{\Pi}}_s + \mathbf{h}_s\right] &= q_s n_s\mathbf{u}_s\cdot\mathbf{E} + \mathcal{C}_s^{[2]} + \mathcal{S}_s^{[2]}.
\end{aligned}$$

Model	Reduction	Index Set
General		$\Lambda_{\mathrm{G}} = \left\{(\alpha,k) : \alpha = 1,\ldots,N_A; k = 0,\ldots,z_\alpha\right\}\cup\{e\}$
Average Ionization	$\sum_{k=1}^{z_\alpha}$	$\Lambda_{\mathrm{I}} = \left\{(\alpha,0) : \alpha = 1,\ldots,N_A\right\}\cup\left\{(\alpha,i) : \alpha = 1,\ldots,N_A\right\}\cup\{e\}$
Average Ion-Neutral	$\sum_{k=0}^{z_\alpha}$	$\Lambda_{\mathrm{IN}} = \left\{\alpha : \alpha = 1,\ldots,N_A\right\}\cup\{e\}$

Analytic Rate Coefficients

Ionization (Voronov): $\Gamma^{\text{ion}}_{(\alpha,k)} = n_e n_{(\alpha,k)} I_{(\alpha,k)}$ with

$$I_{(\alpha,k)} = A_{(\alpha,k)} \frac{1 + P_{(\alpha,k)} \sqrt{U_{(\alpha,k)}}}{X_{(\alpha,k)} + U_{(\alpha,k)}} \left(U_{(\alpha,k)}\right)^{K_{(\alpha,k)}} \exp\left(-U_{(\alpha,k)}\right).$$

Recombination (Badnell): $\Gamma^{\text{rec}}_{(\alpha,k)} = n_e n_{(\alpha,k)} \left(R^{\text{rad}}_{(\alpha,k)} + R^{\text{die}}_{(\alpha,k)}\right)$ with

$$R^{\text{rad}}_{(\alpha,k)} = A_{(\alpha,k)} \left[\sqrt{T_e/T_0^{(\alpha,k)}} \left(1 + \sqrt{T_e/T_0^{(\alpha,k)}}\right)^{1-D_{(\alpha,k)}} \left(1 + \sqrt{T_e/T_1^{(\alpha,k)}}\right)^{1+D_{(\alpha,k)}}\right]^{-1}, \qquad D_{(\alpha,k)} = B_{(\alpha,k)} + C_{(\alpha,k)} \exp\left(-T_2^{(\alpha,k)}/T_e\right),$$

$$R^{\text{die}}_{(\alpha,k)} = T_e^{-3/2} \sum_{i=1}^{N_{(\alpha,k)}} c_i^{(\alpha,k)} \exp\left(-E_i^{(\alpha,k)}/T_e\right).$$

Momentum & Energy Transfer:

$$\mathbf{R}_{s;t} = \alpha_{s;t} \left(\mathbf{u}_t - \mathbf{u}_s\right) \Phi_{s;t}$$
$$Q_{s;t} = \frac{\alpha_{s;t}}{m_s + m_t} \left[A_{s;t} k_{\text{B}} \left(T_t - T_s\right) \Psi_{s;t} + m_t \left(\mathbf{u}_t - \mathbf{u}_s\right)^2 \Phi_{s;t}\right],$$

Charge-charge:

$$\alpha_{s;t} \stackrel{\text{def}}{=} \frac{n_s n_t Z_s^2 Z_t^2 |q_e|^4 \ln \Lambda_{s;t}}{6\pi\sqrt{2\pi}\epsilon_0^2 m_{s;t} \left(k_{\text{B}} T_s/m_s + k_{\text{B}} T_t/m_t\right)^{3/2}},$$

Charge-neutral/Neutral-neutral:

$$\alpha_{s;t} \stackrel{\text{def}}{=} n_s n_t m_{s;t} \frac{4}{3} \left[\frac{8}{\pi} \left(\frac{k_{\text{B}} T_s}{m_s} + \frac{k_{\text{B}} T_t}{m_t}\right)\right]^{1/2} \sigma_{s;t}.$$

Multifluid EM plasma model: Multiple Atomic Species, Full Maxwell/Electrostatic Collisions/Ionization/recombination

Density	$\partial_t \rho_s + \nabla \cdot (\rho_s \mathbf{u}_s) = -\rho_s n_e (I_s + R_s) + m_s n_e (n_{s-1} I_{s-1} + n_{s+1} R_{s+1})$
Momentum	$\partial_t (\rho_s \mathbf{u}_s) + \nabla \cdot (\rho_s \mathbf{u}_s \otimes \mathbf{u}_s + p_s \underline{\mathbf{I}} + \underline{\Pi}_s) = q_s n_s (\mathbf{E} + \mathbf{u}_s \times \mathbf{B}) + \sum_{t \neq s} \alpha_{s;t} \rho_s \rho_t (\mathbf{u}_t - \mathbf{u}_s)$ $-\rho_s \mathbf{u}_s n_e (I_s + R_s) + \frac{m_s}{m_{s-1}} n_e \rho_{s-1} \mathbf{u}_{s-1} I_{s-1} + (n_e \rho_{s+1} \mathbf{u}_{s+1} + n_{s+1} \rho_e \mathbf{u}_e) R_{s+1}$
Energy	$\partial_t \mathcal{E}_s + \nabla \cdot [(\mathcal{E}_s + p_s) \mathbf{u}_s + \mathbf{u}_s \cdot \underline{\Pi}_s + \mathbf{h}_s] = q_s n_s \mathbf{u}_s \cdot \mathbf{E} + \sum_{t \neq s} \frac{\alpha_{s;t} \rho_s \rho_t}{m_s + m_t} [A_{s;t} k_B (T_t - T_s) + m_t (\mathbf{u}_t - \mathbf{u}_s)^2]$ $-\mathcal{E}_s n_e (I_s + R_s) + \frac{m_s}{m_{s-1}} n_e \mathcal{E}_{s-1} I_{s-1} + (n_e \mathcal{E}_{s+1} + n_{s+1} \mathcal{E}_e) R_{s+1}$
Charge and Current	$q = \sum_s q_s n_s$ $\qquad$ $\mathbf{J} = \sum_s q_s n_s \mathbf{u}_s$
Maxwell's Equations	$\frac{1}{c^2} \partial_t \mathbf{E} - \nabla \times \mathbf{B} + \mu_0 \mathbf{J} = \mathbf{0}$ $\qquad$ $\nabla \cdot \mathbf{E} = \frac{q}{\epsilon_0}$ $\partial_t \mathbf{B} + \nabla \times \mathbf{E} = \mathbf{0}$ $\qquad$ $\nabla \cdot \mathbf{B} = 0$

1. Flexible and extensible multi-physics PDE solver framework (**Drekar**) can accommodate arbitrary # species for full multi-fluid models
2. Nodal FE and structure-preserving FE discretizations (edge, face, …)
3. Stable and accurate AFC local bounds preserving CG FE methods
4. IMEX to handle fast physics (e.g. large plasma/cyclotron freq & EM CFL etc.)
5. Robust and scalable nonlinear / linear solvers for CG/structure preserving

   => Newton-Krylov with physics-based / block decomposition prec.
   enabling optimal H(curl) and H(grad) multilevel sub-solvers

Demonstration / Verification of Implicit Solution for Longitudinal Electron Plasma (LEP) Oscillation with Under-resolved TEM Waves

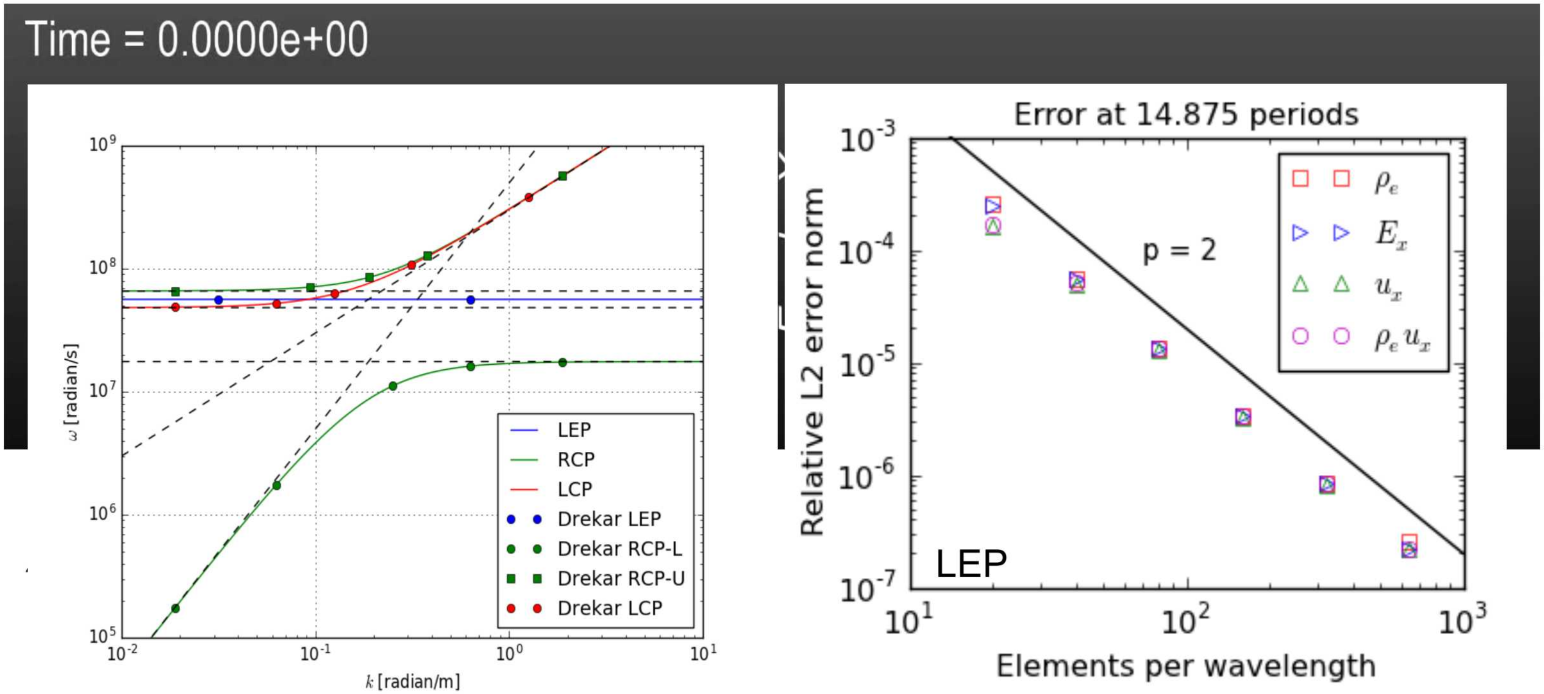

LEP: Longitudinal Electron Plasma Wave
RCP: Right Hand Circularly Polarized Wave
LCP: Left Hand Circularly Polarized Wave
(Cold plasma)

Verification effort with Niederhaus, Radtke, Bettencourt, Cartwright, Kramer, Robinson and ATDM EMPIRE Team

Robustness and Accuracy: Asymptotic IMEX Solution of Full Multifluid EM Plasma Model in MHD Limit (Visco-resistive Alfven Wave)

Implicit L-stable and IMEX SSP/L-stable time integration and block preconditioners enable solution of multifluid EM plasma model in the asymptotic resistive MHD limit.

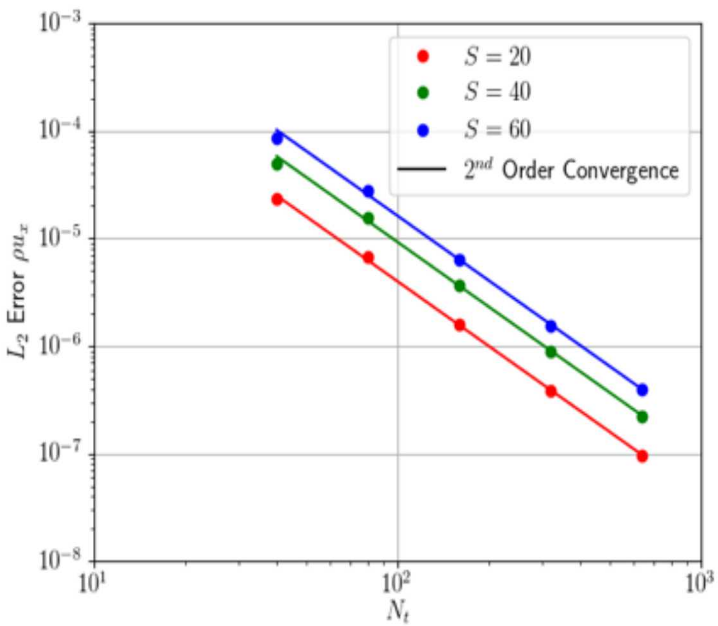

Accuracy in MHD limit (IMEX)

Plasma Scales for S = 60		
	Electrons	**Ions**
$\omega_p \Delta t$	10^7 - 10^9	10^6 - 10^7
$\omega_c \Delta t$	10^6 - 10^7	10^3 - 10^4
$\nu_{\alpha\beta} \Delta t$	10^{10} - 10^{11}	10^7 - 10^8
$\nu_S \Delta t / \Delta x$	10^{-2}	10^{-4}
$u \Delta t / \Delta x$	10^{-4}	10^{-4}
$\mu \Delta t / \rho \Delta x^2$	10^{-1} - 10^{1}	10^{-2} - 10^{0}
$c \Delta t / \Delta x$	10^2	

IMEX terms: implicit/explicit

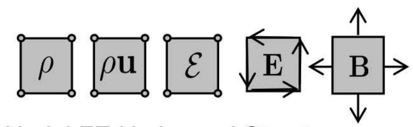

Nodal FE Hydro and Structure-preserving discretization for EM

Implicitly overstepping stiff modes, not controlling accuracy, can make an intractable explicit computation – tractable with IMEX methods.

Overstepping fast time scales is both stable and accurate. The inclusion of a resistive operator adds dissipation to the electron dynamics on top of the L-stable time integrator.

Verification of Collisional Transfer: Analytic Damped EM Plasma Oscillations in Drekar;

$$\mathbf{u}_e(t)-\mathbf{u}_i(t)=\left(\mathbf{u}_e(t_0)-\mathbf{u}_i(t_0)\right)\exp\left(-\frac{\nu_{e;i}t}{2}\right)\frac{\cos\left(\eta_{e;i}t-\phi_{e;i}\right)}{\cos\phi_{e;i}},$$

$$\mathbf{E}(t)=-\left(\mathbf{u}_e(t_0)-\mathbf{u}_i(t_0)\right)\frac{q_e n_i}{\epsilon_0}\frac{\exp\left(-\nu_{e;i}t/2\right)}{\omega_{e;i}^2\cos\phi_{e;i}}\left[\eta_{e;i}\sin\left(\eta_{e;i}t-\phi_{e;i}\right)-\frac{\nu_{e;i}}{2}\cos\left(\eta_{e;i}t-\phi_{e;i}\right)\right.$$
$$\left.+\exp\left(\nu_{e;i}t/2\right)\left(\frac{\nu_{e;i}}{2}\cos\phi_{e;i}+\eta_{e;i}\sin\phi_{e;i}\right)\right].$$

$$T_e(t)-T_i(t)=\exp\left(-A_{e;i}t\right)C_{e;i}+\frac{D_{e;i}\exp\left(-\nu_{e;i}t\right)}{\cos^2\phi_{e;i}}\left[4\eta_{e;i}^2+2\left(A_{e;i}-\nu_{e;i}\right)^2\cos^2\left(\eta_{e;i}t-\phi_{e;i}\right)\right.$$
$$\left.+4\eta_{e;i}\left(A_{e;i}-\nu_{e;i}\right)\sin\left(\eta_{e;i}t-\phi_{e;i}\right)\cos\left(\eta_{e;i}t-\phi_{e;i}\right)\right]$$

Mass:	m_i = 2.0e-27, n_e = 1.0e-27
Number density:	n_i = n_e = 2.0e+16
Initial velocity:	v_i = 1.0e+4, v_e = -1.4e+4
Initial Temperature	T_i = 1.0e+4, T_e = 2.0e+4

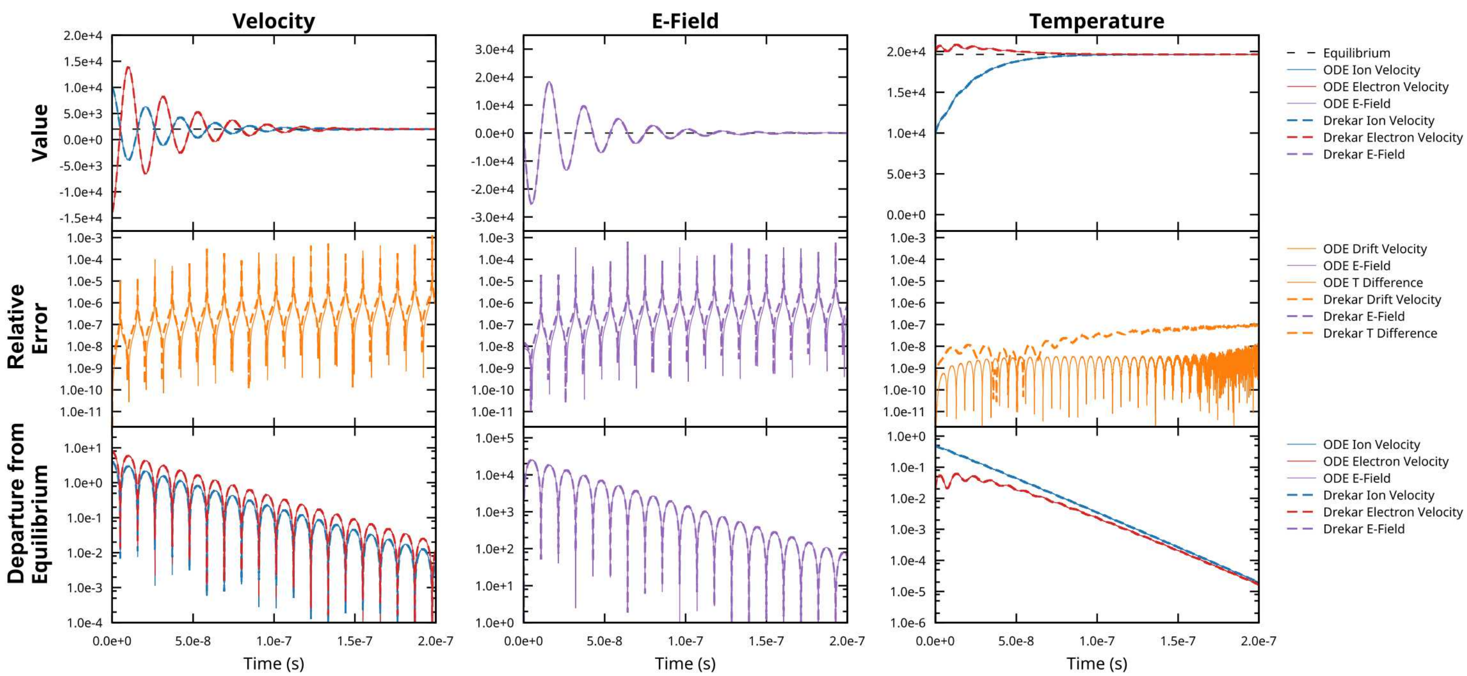

Developing an initial analytic ionization/recombination model for Drekar (to use with AD). Evaluation of Ionization: Voronov and Recombination: Badnel (low density limit)

Charge level populations

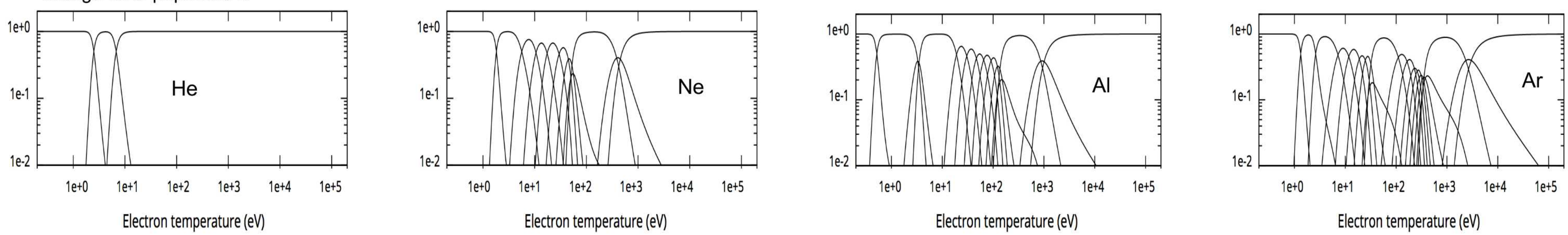

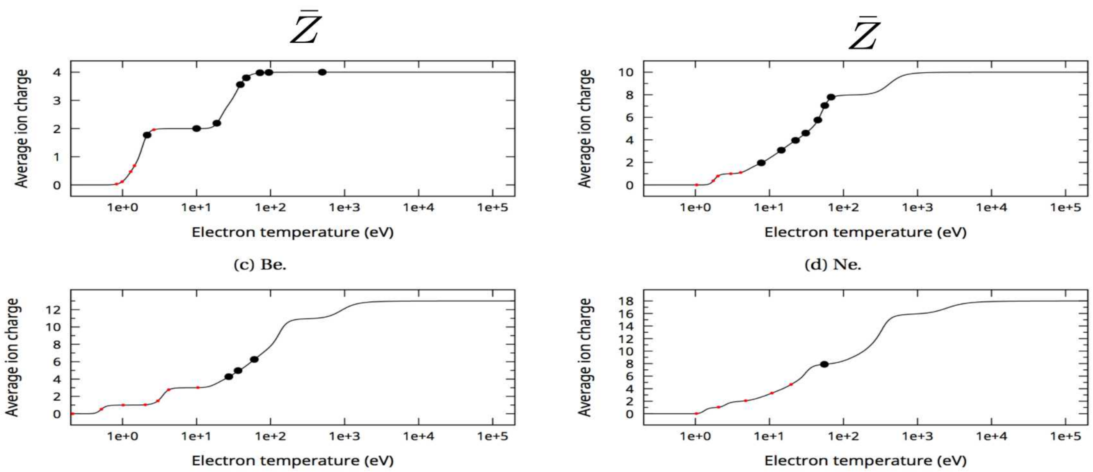

(c) Be. (d) Ne.

(e) Al. (f) Ar.

Figure 9: Each figure compares the equilibrium ionization state of the elements H, He, Be, Ne, Al, Ar from different sources. Sources include: (i) equilibrium computed directly from CIE Python script (solid line), and (ii) equilibrium values computed through time-dependent Drekar simulation using either all possible charge states (black dots) or a reduced set of charge states (red dots).

Highlight: High Z gas transport, ionization, and recombination with multifluid model

- In a disruption, plasma temperature will drop from 10 keV to a few eV in a few ms.
- This energy can be mostly channeled through runaway electrons.
- Complete avoidance is impractical
- Optimal scenario is to avoid runaway avalanche

- Goal: Guide / moderate tokamak disruption thermal quench, and runaway electron avalanche, with radiative cooling and low-energy electrons from high Z impurities.

- Preliminary proof-of-principle 1D study of a core of 0.1 eV, $n = 10^{24}$ Ne^0, Ar^0 neutral gases expanding in a 100eV, $n = 10^{20}$ Deuterium plasma. Profiles at t = 1 microsecond.

<u>Disruption is a prompt termination of a plasma confinement in a tokamak and can be a showstopper for ITER. Mitigate to control thermal and current quench evolution.</u>

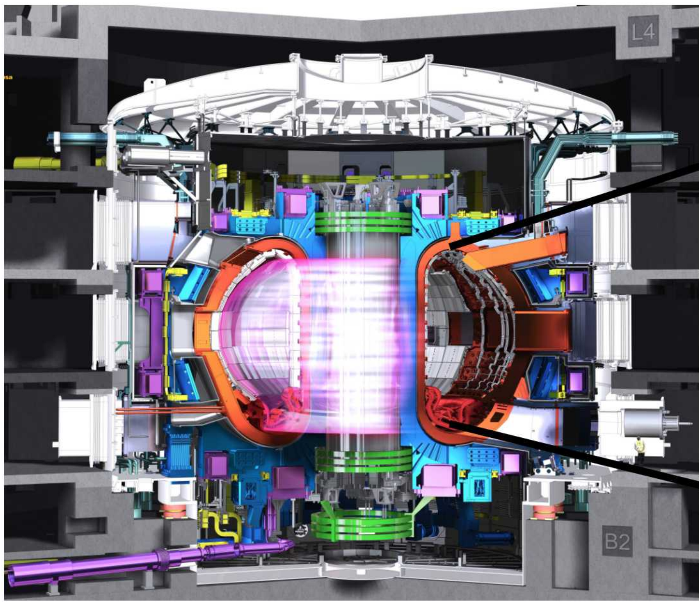

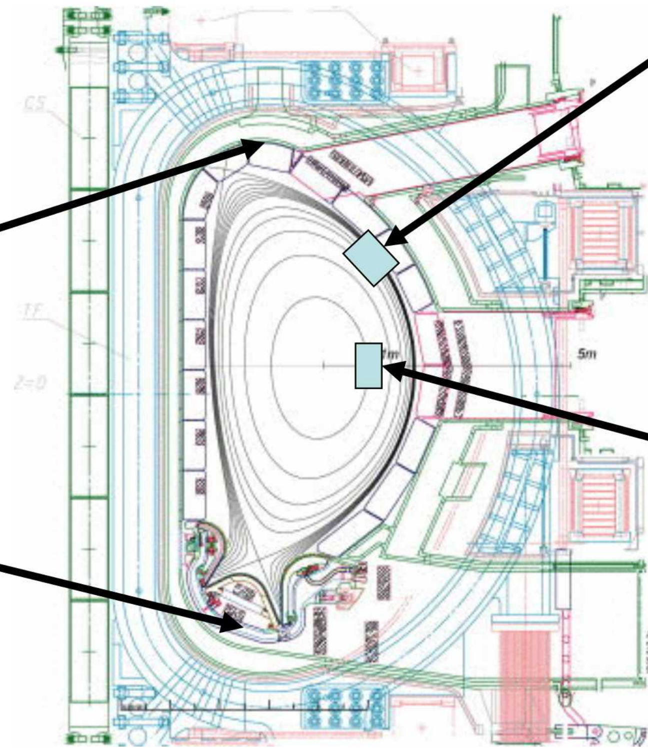

ITER Project: https://www.iter.org/

DOE Advanced Scientific Computing Research (ASCR) / Office of Fusion Energy (OFES)
SciDAC Partnership: Tokamak Disruption Simulation (TDS) Project

<u>Preliminary Models of Gas Injection for Disruption Mitigation</u>

<u>Dynamics of Neutral Gas Jet Injection at an angle wrt B Field</u>

- Hydrodynamics of jet
- Collisional effects
- Ionization/recombination
  - E field interactions for charged species
  - Interactions with B field for charged species

<u>Gas Injection Assumed Distribution at time t= 0 for Neutral Gas Core Inside Separatrix</u>

- Hydrodynamics of neutral core expansion
- Collisional effects
- Ionization/recombination
  - E field interactions for charged species
  - In 2D,3D interactions with B field for charged species

A Very Preliminary 1D Gas Injection Related Problem

1D High Z Neutral Gas (Ne0) Core Expansion into a 100ev Deuterium (D+,e-) Plasma

Solving Conservation of Mass, Momentum, Total Mech. Energy
(i.e. Euler sub-system with collisions / ionization / recombination and EM forces) for

$$(D^0, D^{1+}, Ne^0, Ne^{1+}, Ne^{2+}, Ne^{3+}, Ne^{4+}, e^-)$$

and electromagnetics for (E,B).

5 moment plasma model x 8 species	= 40 equations	(solved in 3D but only a 1D solution)
Maxwell Equations E,B field	= 6 equations	(solved in 3D but only a 1D solution)

<u>Problem outline:</u>

- Initial ~fully ionized Deuterium plasma at n = 10^{20}, T = 100ev (~1M degrees K)
- Neutral Neon (Ne^0) core introduced at n = 10^{22} , T = 10^{-1}ev (~1000 degrees K)
- Parallel B – field is ignorable (due to geometry in 1D so B does not modify transport)
- Mesh 4096x1x1 elements

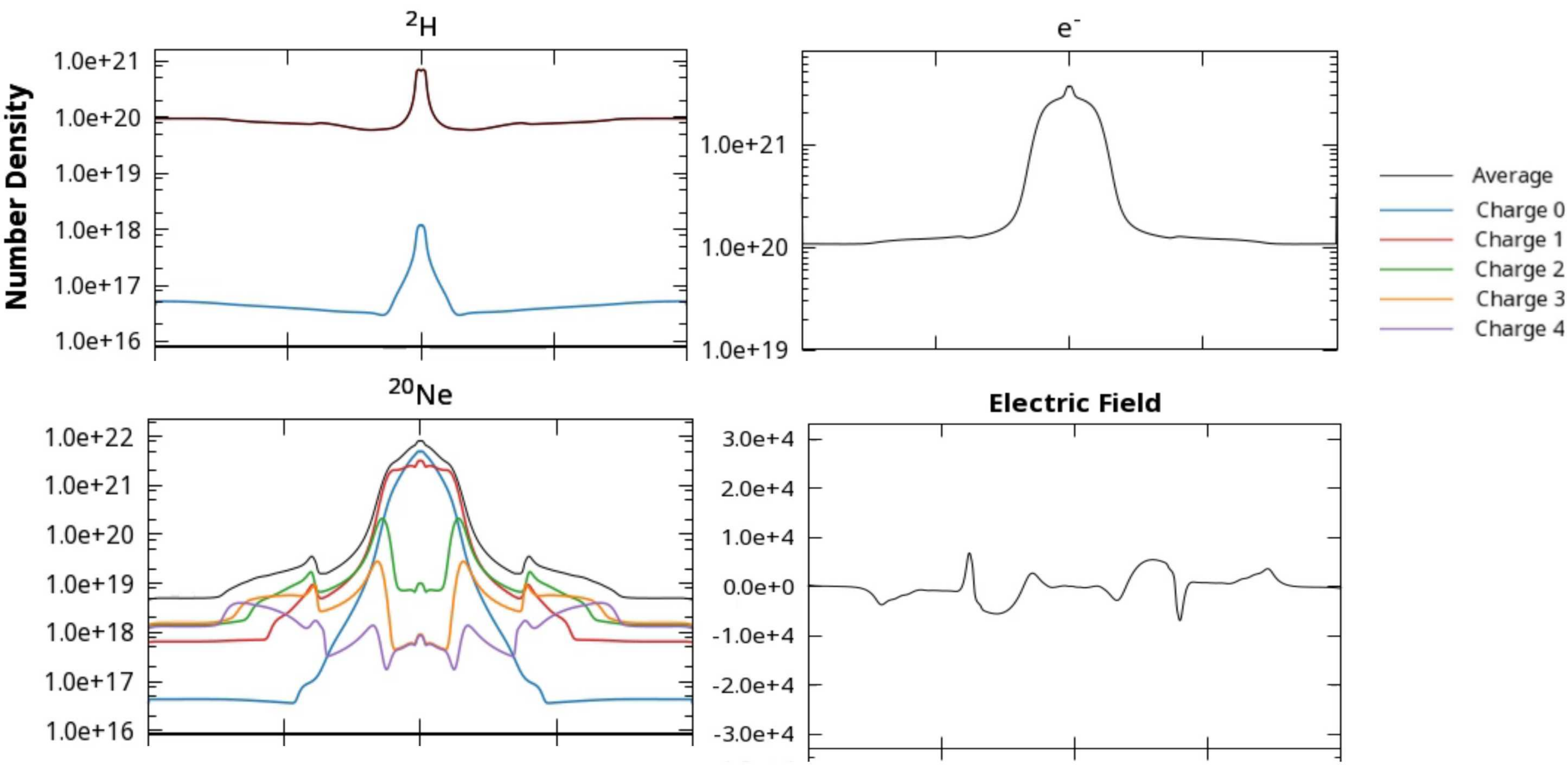

²H
e⁻
²⁰Ne
Electric Field
Number Density
1.0e+21
1.0e+20
1.0e+19
1.0e+18
1.0e+17
1.0e+16
1.0e+22
3.0e+4
2.0e+4
1.0e+4
0.0e+0
-1.0e+4
-2.0e+4
-3.0e+4
Average
Charge 0
Charge 1
Charge 2
Charge 3
Charge 4

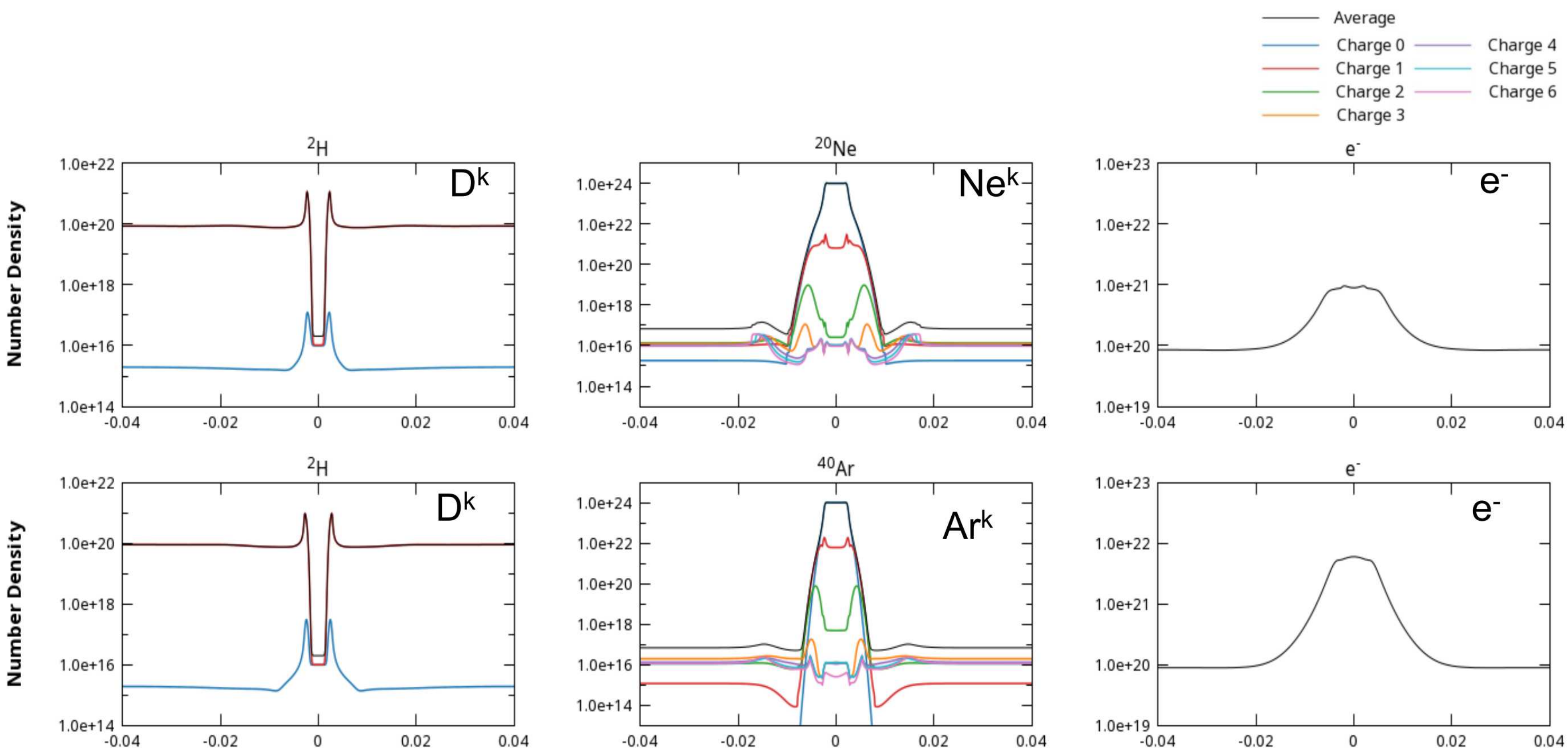

Average
Charge 0
Charge 1
Charge 2
Charge 3
Charge 4
Charge 5
Charge 6
^{2}H
D^k
^{20}Ne
Ne^k
e$^-$
e^-
^{40}Ar
Ar^k
Number Density
1.0e+22
1.0e+20
1.0e+18
1.0e+16
1.0e+14
1.0e+24
1.0e+23
1.0e+21
1.0e+19
-0.04
-0.02
0
0.02
0.04

Coarse mesh (100x100x100) early time 3D image of a 3D simulation.
It is for 0.1ev He0 in a (D+,e-) 100ev Plasma. The B field is static and 1T.
The simulation has collisions/ionization/recombination for (e-,D0,D1+,He0,He1+,He2+).

The image shows a iso-surface of the magnitude of momentum for both He0 (isotropic expansion) and e- (anisotropic expansion).
The e- momentum surface is colored by electron density.

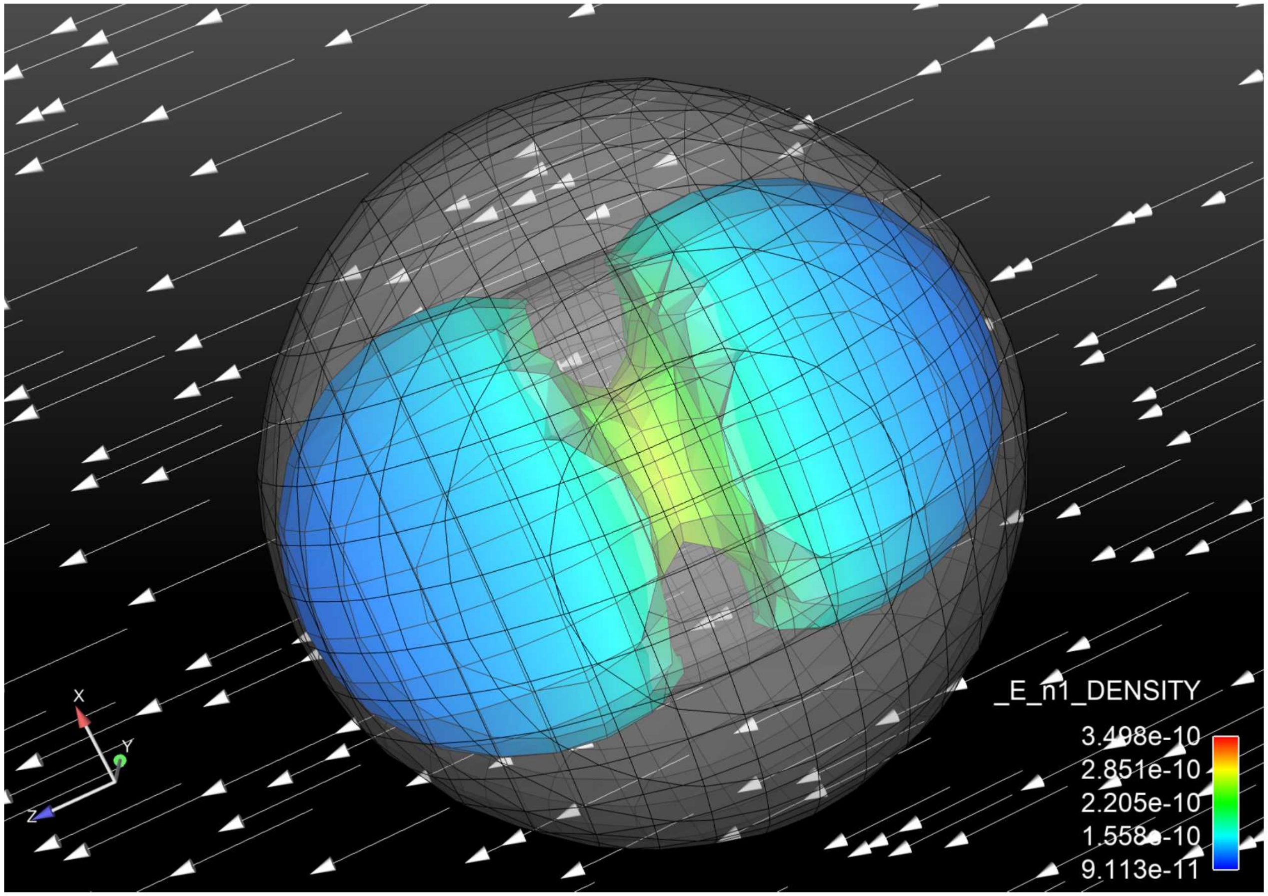

Coarse mesh (100x100x100) early time 3D image of a 3D simulation.
It is for 0.1ev He0 in a (D+,e-) 100ev Plasma. The B field is static and 1T.
The simulation has collisions/ionization/recombination for (e-,D0,D1+,He0,He1+,He2+).

The image shows a iso-surface of the magnitude of momentum for both He0 (isotropic expansion) and e- (anisotropic expansion).
The e- momentum surface is colored by electron density.

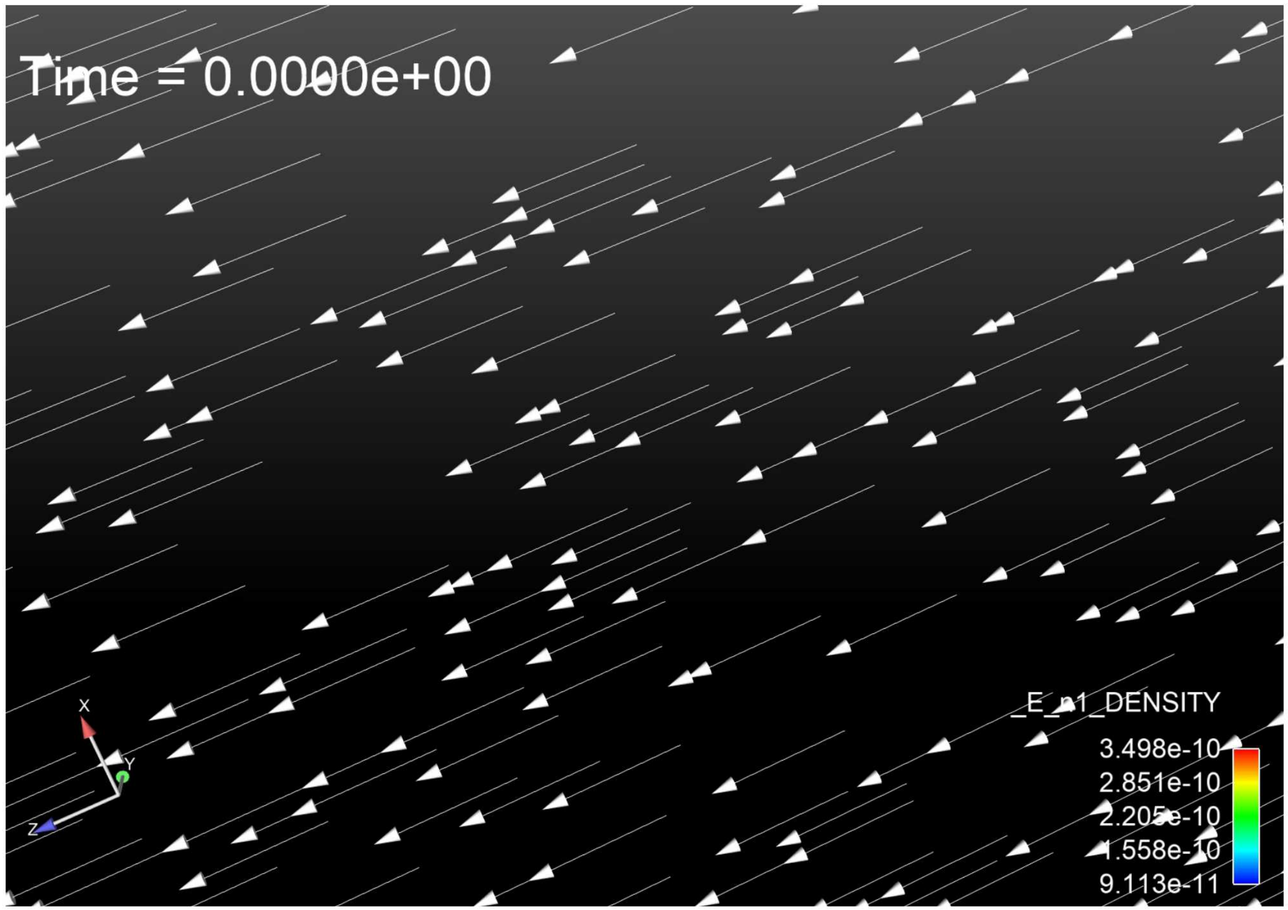

Coarse mesh (100x100x100) early time 3D image of a 3D simulation.
It is for 0.1ev He0 in a (D+,e-) 100ev Plasma. The B field is static and 5T.
The simulation has collisions/ionization/recombination for (e-,D0,D1+,He0,He1+,He2+).

The image shows a iso-surface of the magnitude of momentum for both He0 (isotropic expansion) and e- (anisotropic expansion).
The e- momentum surface is colored by electron density.

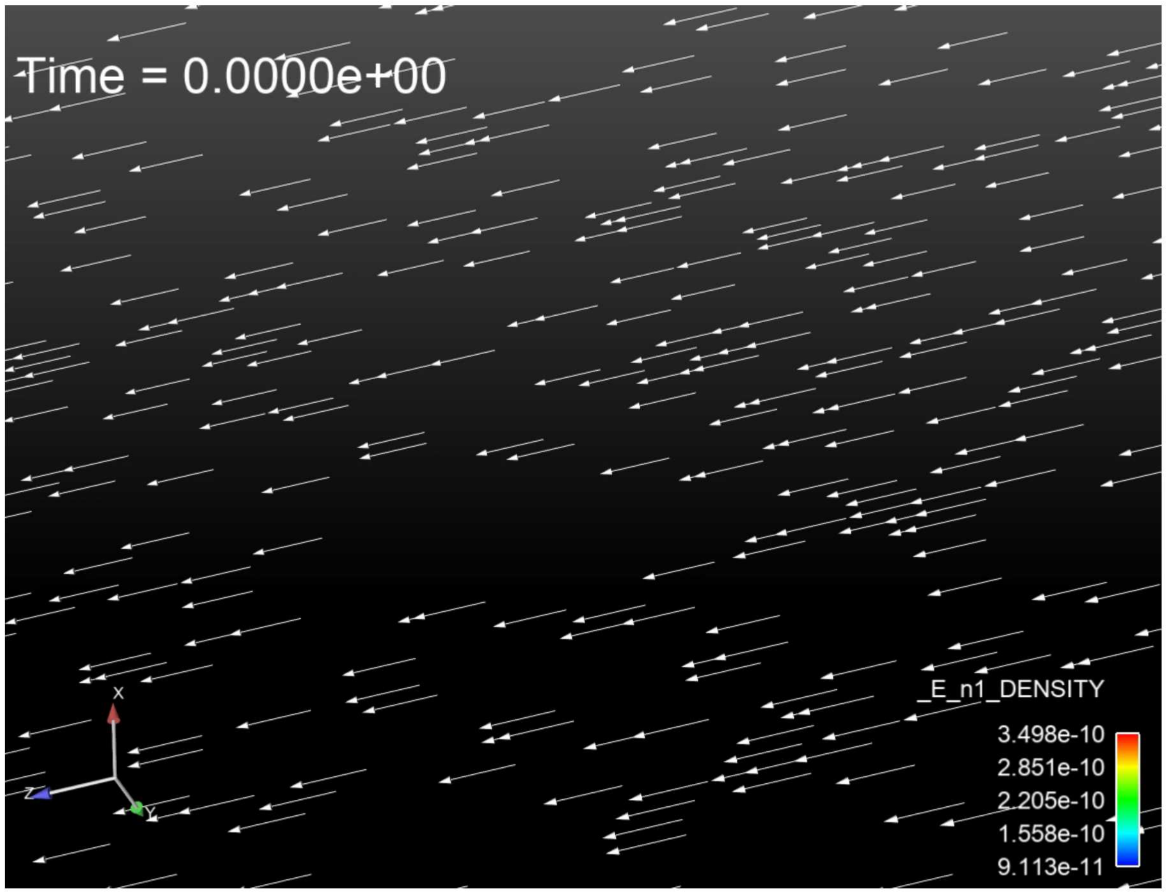

Overview

- Numerical Model
  - Multifluid
  - Kinetic
- Expanding slab
  - Base case: $n_0 = 10^{16}$
  - Density variation: $10^{10} < n_0 < 10^{22}$
  - Run time comparisons
- Neutral gas injection
  - Collision models
  - Comparisons

Multifluid Model

- Conservation equations for species s

$$\partial_t \rho_s + \nabla \cdot \rho \mathbf{v}_s = \mathcal{C}_s^{[0]} + \mathcal{S}_s^{[0]} \tag{1}$$

$$\partial_t(\rho_s \mathbf{v_s}) + \nabla\cdot(\rho \mathbf{v}_s \otimes \mathbf{v}_s + p_s \underline{\mathbf{I}} + \underline{\mathbf{\Pi}}_s) = q_s n_s(\mathbf{E} + \mathbf{v}_s \times \mathbf{B}) + \mathcal{C}_s^{[1]} + \mathcal{S}_s^{[1]} \tag{2}$$

$$\partial_t \mathcal{E}_s + \nabla \cdot [(\mathcal{E}_s + p_s)\mathbf{v}_s + \mathbf{v}_s \cdot \underline{\mathbf{\Pi}}_s + \mathbf{h}_s] = q_s n_s \mathbf{v}_s \cdot \mathbf{E} + \mathcal{C}_s^{[2]} + \mathcal{S}_s^{[2]}, \tag{3}$$

- Maxwell's equations $\rightarrow$ electrodynamic

$$\frac{1}{c^2}\partial_t \mathbf{E} - \nabla \times \mathbf{B} + \mu_0 \mathbf{J} = \mathbf{0} \tag{4}$$

$$\partial_t \mathbf{B} + \nabla \times \mathbf{E} = \mathbf{0} \tag{5}$$

$$\nabla \cdot \mathbf{E} = \frac{q}{\epsilon_0} \tag{6}$$

$$\nabla \cdot \mathbf{B} = 0 \tag{7}$$

- Electrostatic approximation

$$\nabla \cdot \nabla \phi = \frac{q}{\varepsilon_0} \tag{8}$$

Kinetic Model

$$\partial_t f_s + \mathbf{v} \cdot \nabla_{\mathbf{x}} f_s + \frac{q_s}{m_s}(\mathbf{E} + \mathbf{v} \times \mathbf{B}) \cdot \nabla_{\mathbf{v}} f_s = \mathcal{C}_s[f_s] + \mathcal{S}_s. \tag{9}$$

$$f_s = f_s(\mathbf{x}, \mathbf{v}, t) \tag{10}$$

- Electrostatic approximation

$$\nabla \cdot \nabla \phi = \frac{q}{\varepsilon_0} \tag{11}$$

Expanding Slab

- Quasi-neutral plasma expanding into a vacuum

$$n_e = n_i = \begin{cases} n_0 & |x| < L/20 \\ n_0 \times 10^{-6} & |x| \geq L/20 \end{cases} \mathrm{m}^{-3}$$

$$T_e = 10000\,\mathrm{K},\, T_i = 10\,\mathrm{K}$$

- Number densities: $10^{10} < n_0 < 10^{22}$
- Taken to be collisionless
- Advanced to a time of $t = 5 \times 10^{-9}\,\mathrm{s}$
- Comparison of mutlifluid to kinetic approach

Base Case Convergence: $n_0 = 10^{16}$

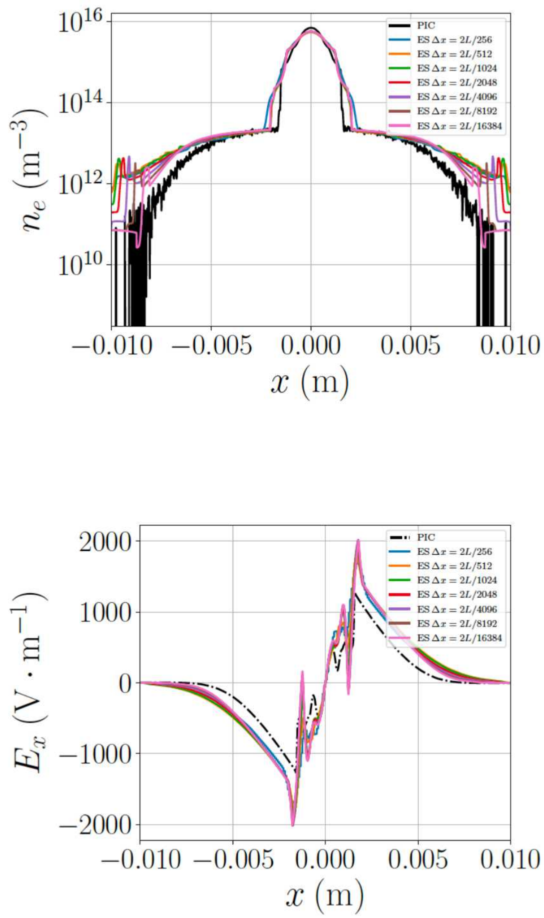

(a) Electrostatic

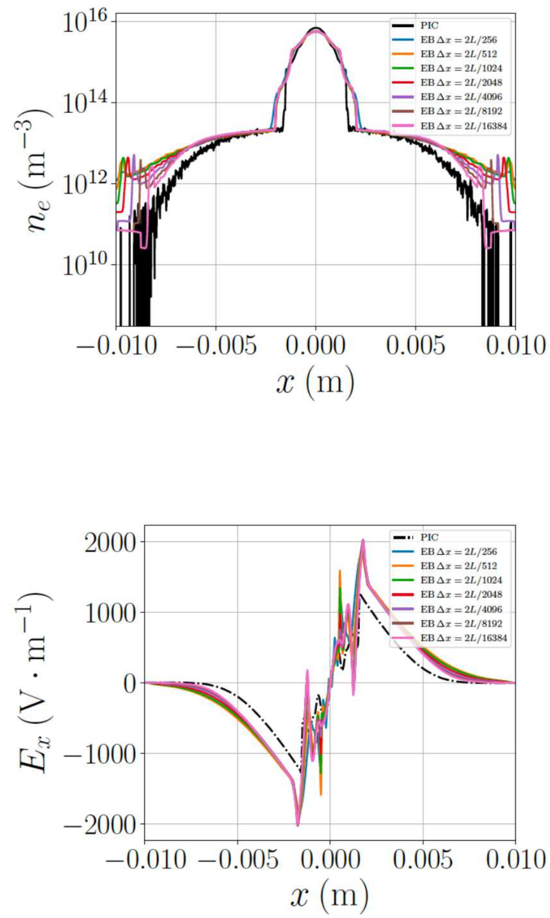

(b) Electrodynamic

Base Case Model Comparison

- Good agreement between the two models for number density
- Other profiles show similar agreement
- However, not fully converged in low density regions as evidenced by previous
- Overall reasonable agreement between the PIC and Fluid models is observed

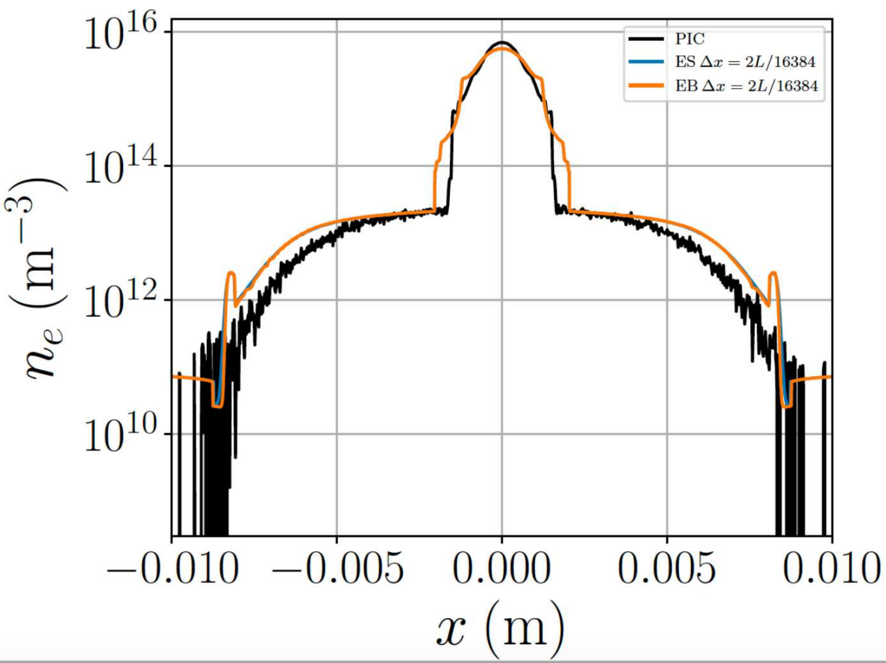

Density Comparisons

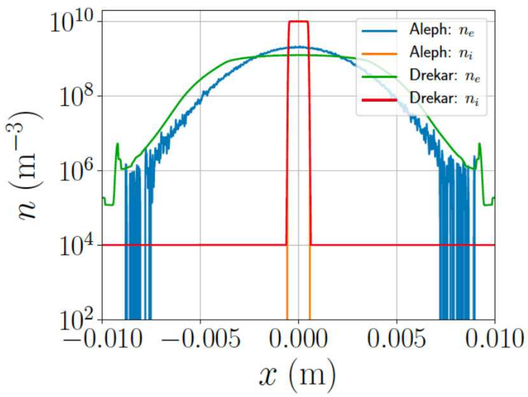

(a) $n_0 = 10^{10}$

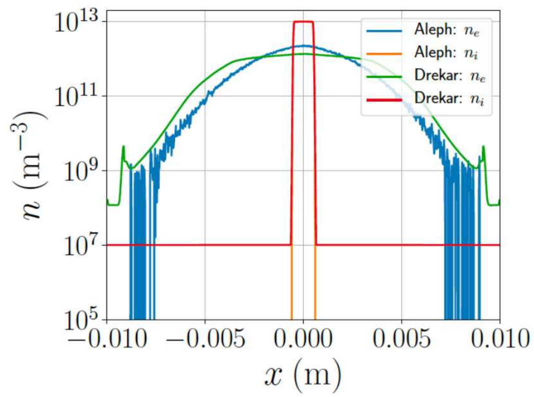

(b) $n_0 = 10^{13}$

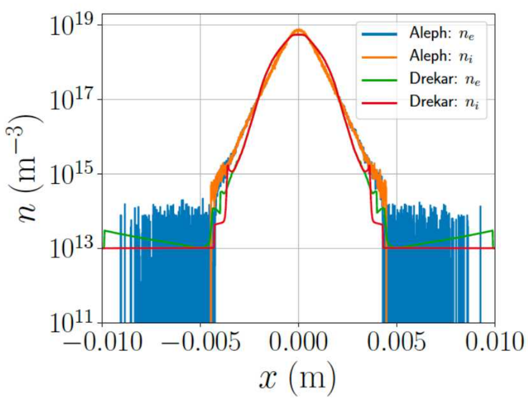

(c) $n_0 = 10^{19}$

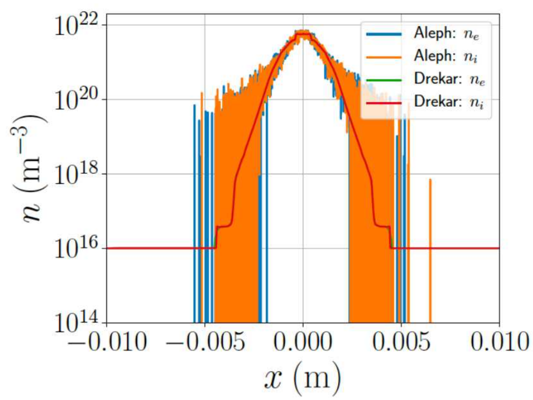

(d) $n_0 = 10^{22}$

Density Comparisons

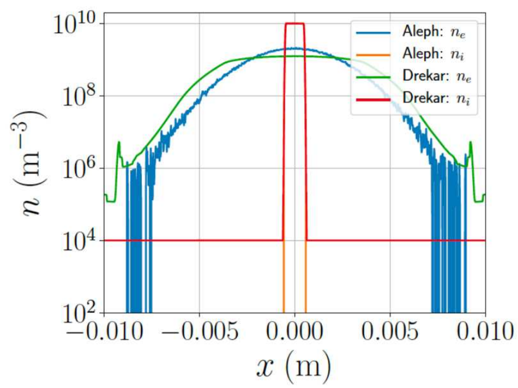

(a) $n_0 = 10^{10}$

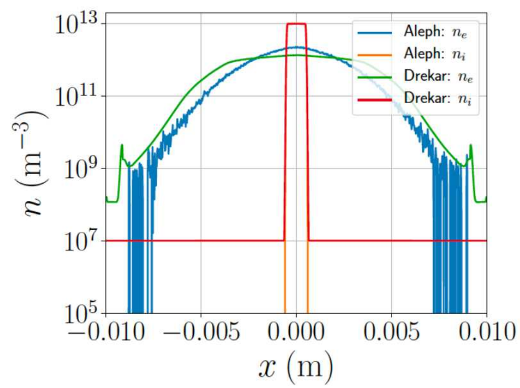

(b) $n_0 = 10^{13}$

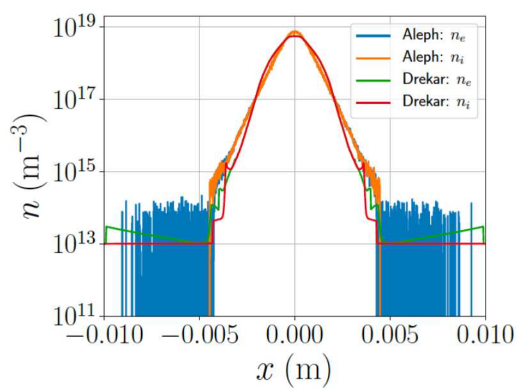

(c) $n_0 = 10^{19}$

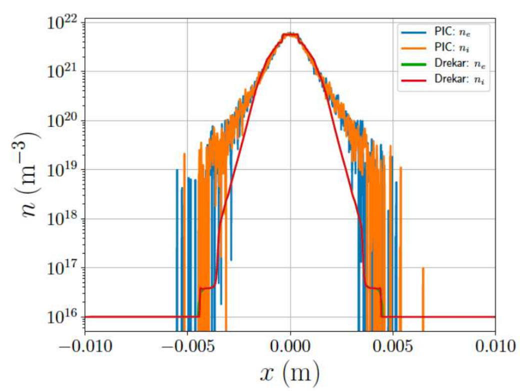

(d) $n_0 = 10^{22}$

Neutral Gas Injection

- Neutral gas injection into $^{2}\mathrm{H}$ plasma
- Initial Conditions:

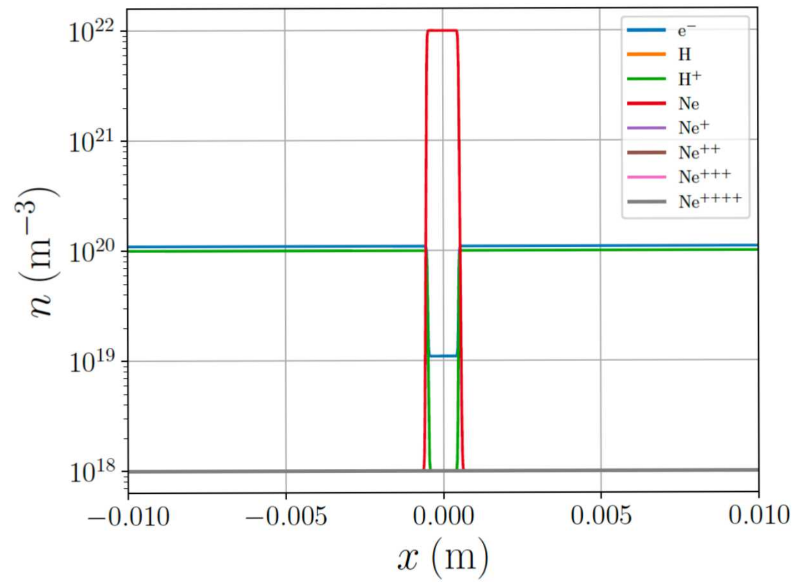

- Collision models:
  - Elastic scattering: hard spheres with same cross-section
  - Coulomb collisions: coulomb logarithm set to 10
  - Ionization: Different rates (cross-section vs rate coefficient)
  - Recombination: Off (PIC currently limited to a constant rate)

Ionization Rate Comparison

- Comparison of rate coefficients in PIC (Lennon) and Drekar (Voronov)
- Rate coefficients for PIC obtained:

$$\langle \sigma v \rangle = \left(\frac{8kT}{\pi m_e}\right)^{1/2} \int_{1/kT}^{\infty} \sigma(E) \frac{E}{kT} \exp\left(\frac{-E}{kT}\right) d\left(\frac{E}{kT}\right)$$

- Decent agreement below 100 eV with some difference in first ionization

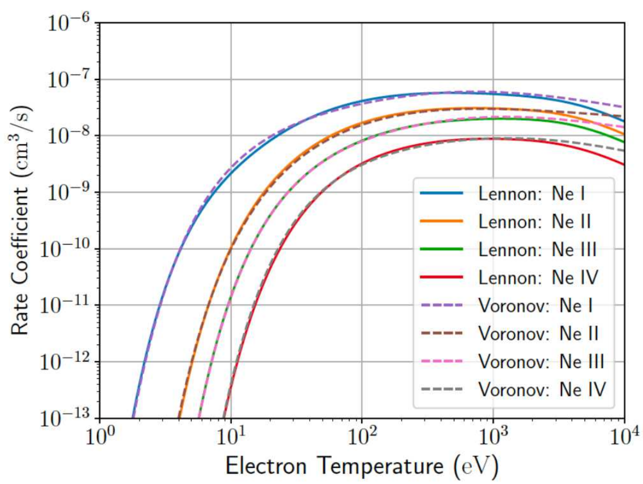

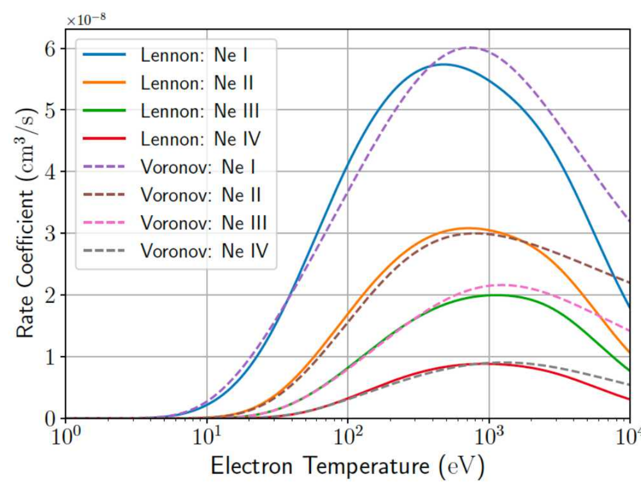

Simulation Comparisons

- $t = 2.0 \times 10^{-8}$ s

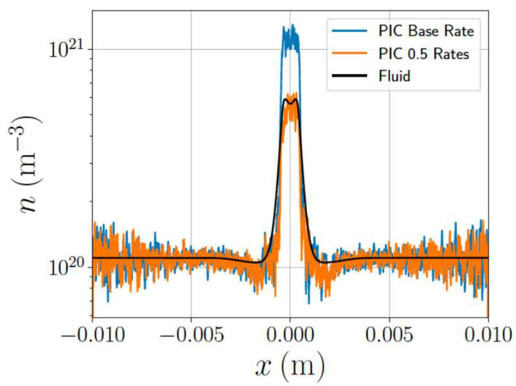

(a) e^{-}

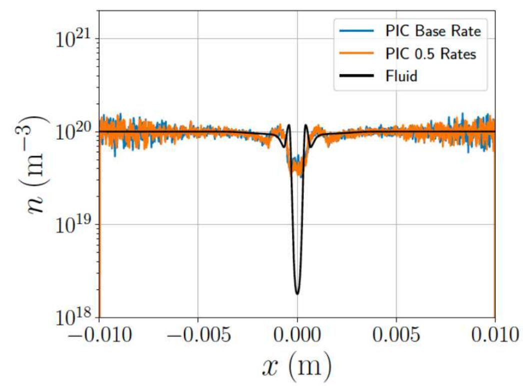

(b) $^{2}H^{+}$

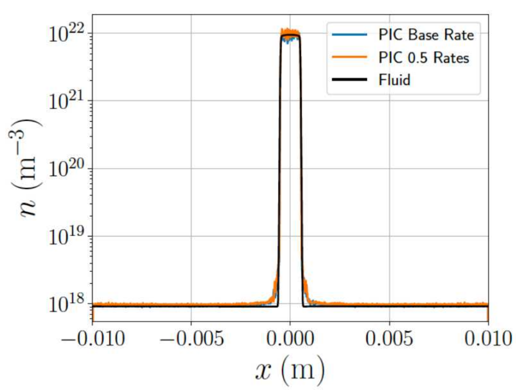

(c) Ne

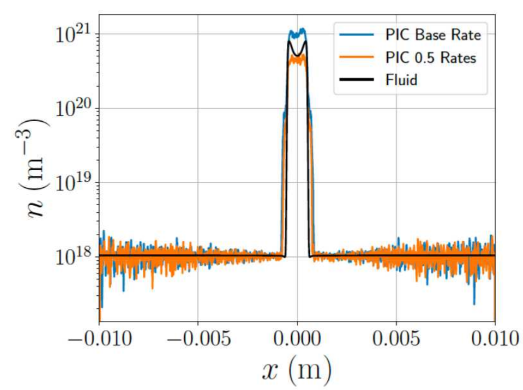

(d) Ne^{+}

Simulation Comparisons

- $t = 4.0 \times 10^{-8}$ s

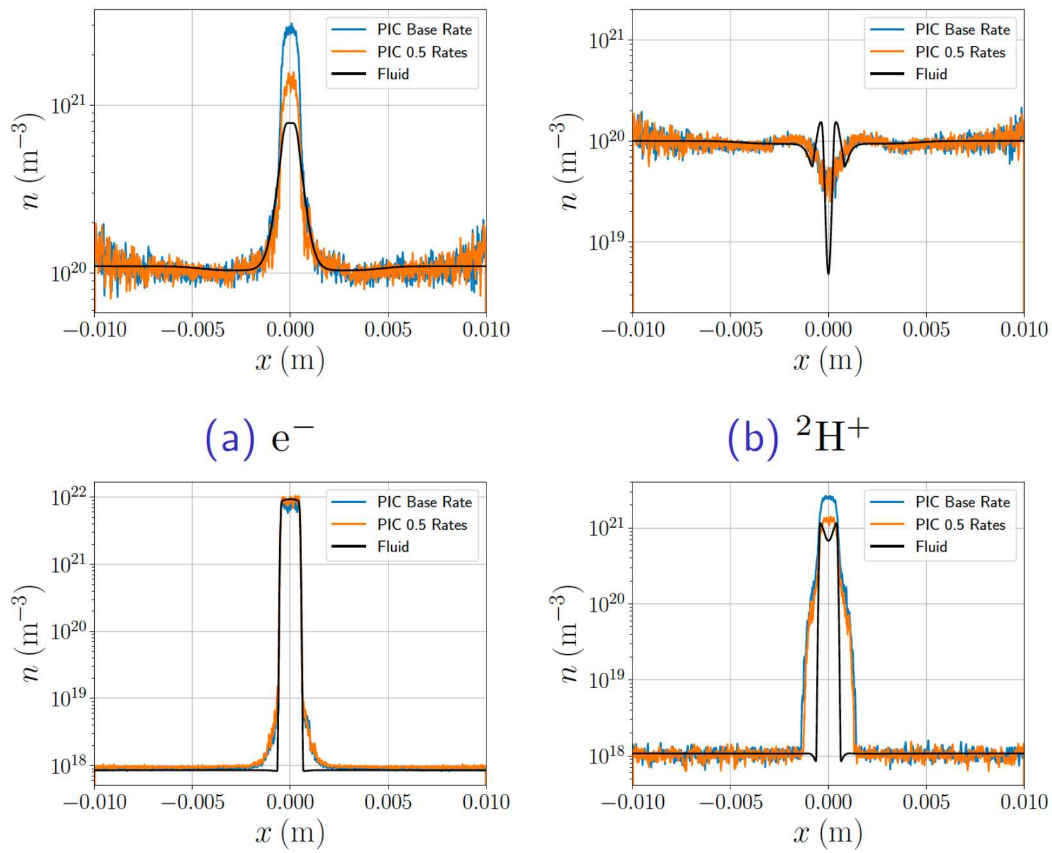

(a) e^- (b) $^2H^+$ (c) Ne (d) Ne^+

Simulation Timings

- Fluid approach is significantly faster at considered number densities
- Extends trends seen in expanding slab ($n_0 = 10^{24}$)
- Relatively fine grid and timestep required for PIC
- Fluid code has smaller grid and larger timestep
- Timings to $4.0 \times 10^{-8}\,\mathrm{s}$

Drekar CPU Hours	PIC CPU Hours
67.2	11500

Highlight: Uncertainty Quantification (UQ)

Development of robust UQ using efficient sampling, surrogate / reduced order modeling (ROM), machine learning, and multilevel/multifidelity approaches, for sensitivities, forward UQ, and inverse UQ for data-informed model improvement.

Exploring multi-level and multi-fidelity methods to reduce the burden on high-fidelity models.

(1) Only ~O(10)-O(100) high-fidelity sims. might be possible,

(2) Low fidelity models often predictive of basic trends,

(3) Plasma physics has a natural model hierarchy (resistive MHD, extended MHD, multifluid, kinetic e.g. PIC),

(4) Can we leverage low-fidelity models in mathematically / statistically rigorous manner?

Beginning Comparisons of Multifluid with PIC: collisionless; Underway collisional/ionization/recombination
Explore fluid/PIC in context of multifidelity UQ in next step

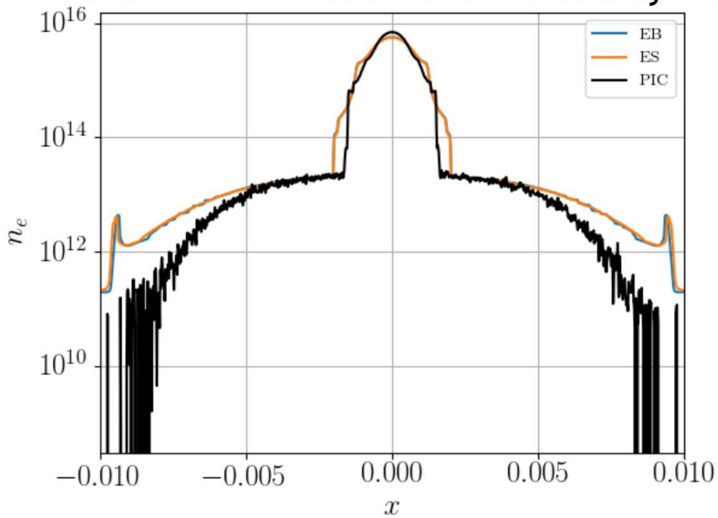

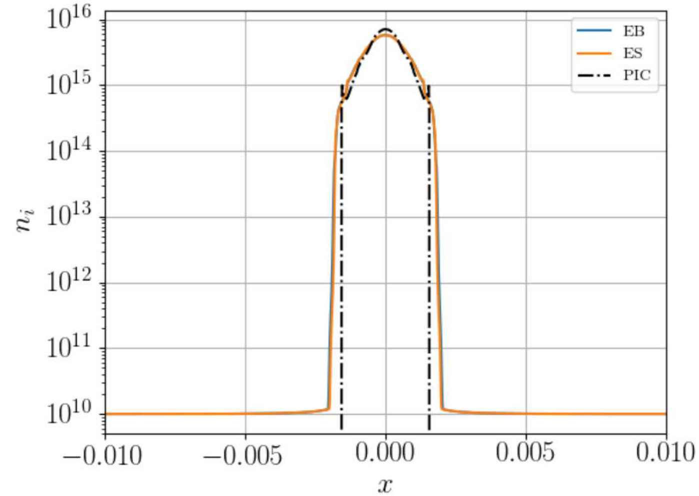

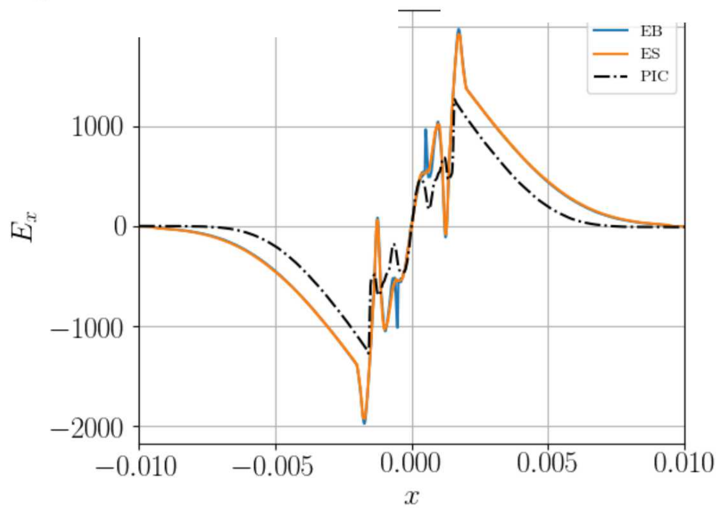

Understanding Fundamental Process and Physical Time-scales in Magnetic Reconnection

Thin Current Sheet Tearing Mode Instability

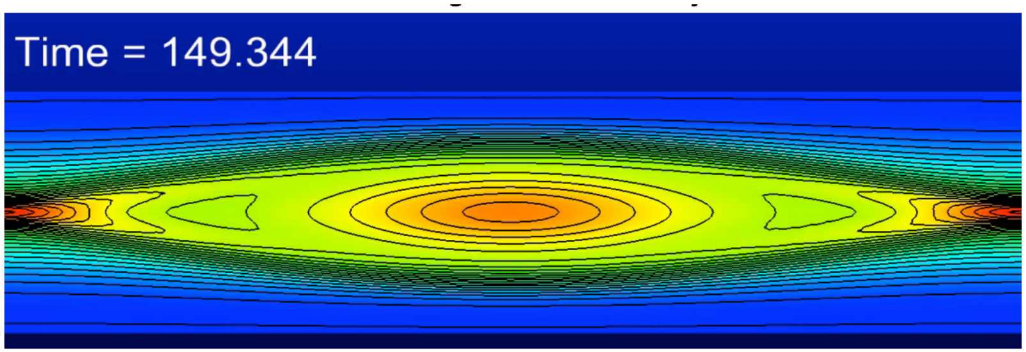

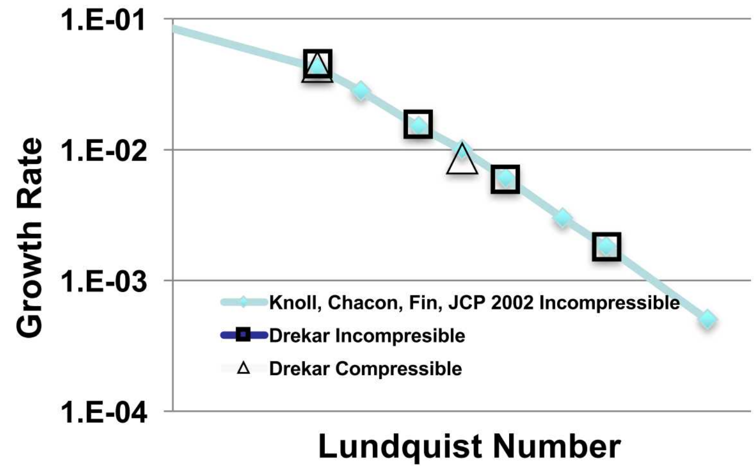

Magnetic Reconnection in Island Coalescence

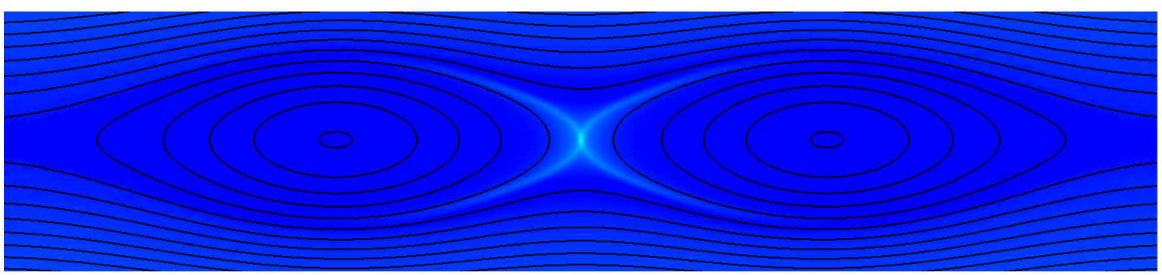

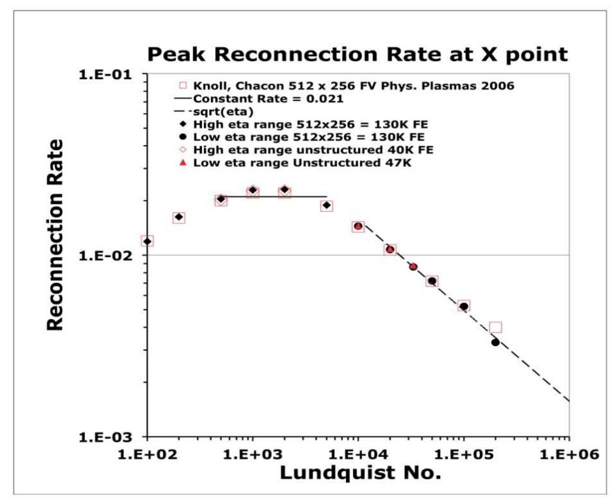

Multi-level UQ Study with FASTMATH UQ SciDAC team
Auto-encoder Neural Net Reduced order modeling (ROM) with RAPIDS SciDAC team

Underway as proof-of-principle:
2D resistive tearing mode
(resistivity and viscosity for now)

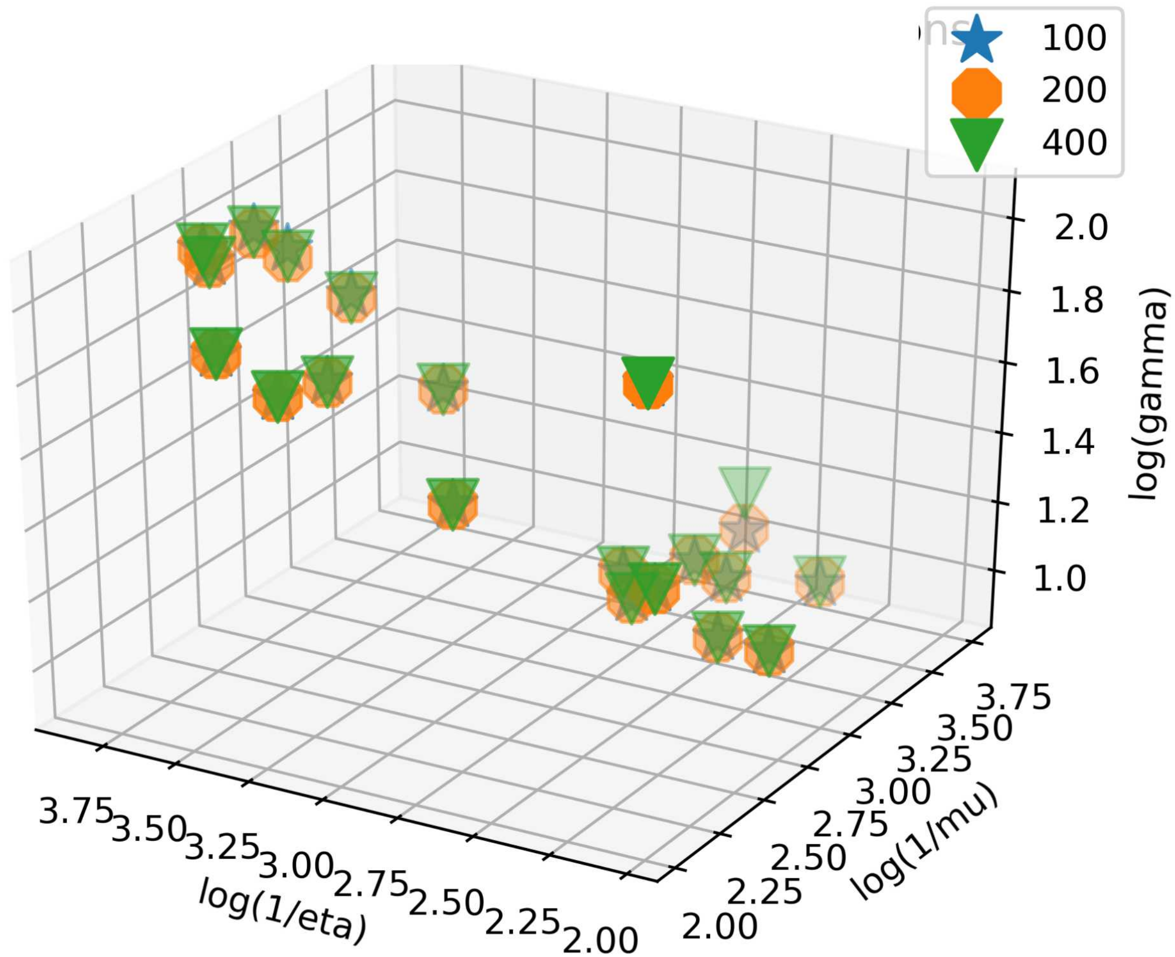

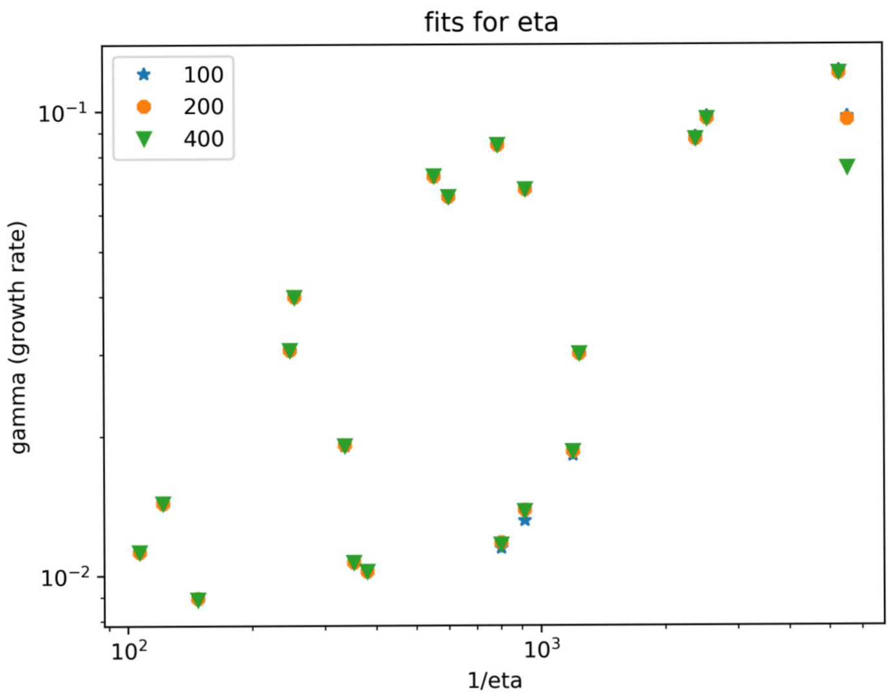

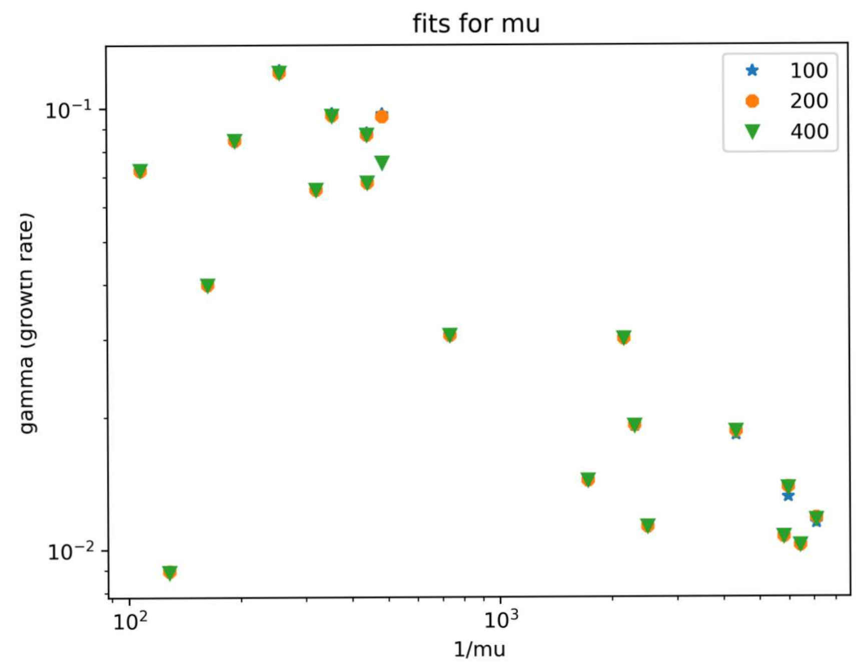

Hopefully initial UQ results will be available.

E.g. Multilevel Monte-Carlo (MLMC) Methods for Efficient UQ

2D Resistive MHD Tearing Mode. Estimates of accuracy and cost of simulations are obtained with exploratory studies, then MLMC defines efficient sequence of computations to either (1) minimize cost for a given accuracy, or (2) maximize accuracy at a fixed cost, for estimated statistical QoI.
(Preliminary results with FASTMATH UQ SciDAC team.)

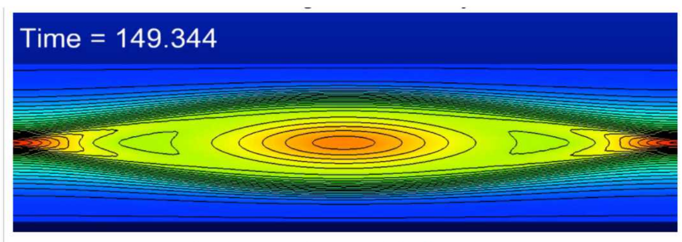

Mesh	Normalized cost
400 x 400	1.0
200 x 200	0.1844
100 x 100	0.0307

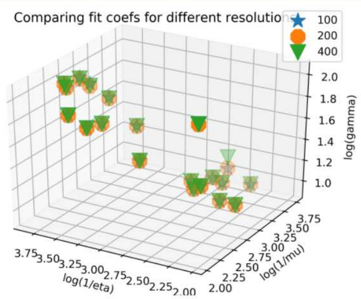

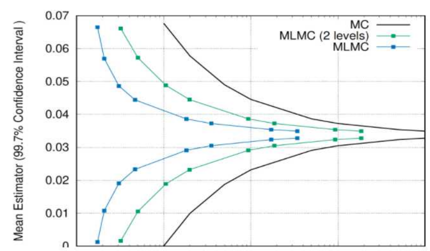

Estimator	N_{400}	N_{200}	N_{100}	Eq. Cost
MC	1273	-	-	1273
MLMC (2 levels)	1	1278	-	236.62
MLMC	1	8	1366	44.36

TABLE: Samples allocation per model and total equivalent cost corresponding to an estimator standard deviation equal to $1E-3$